ANALYSIS OF HEAT TRANSFER ON FLOW OF A NANOFLUID IN A POROUS MEDIUM WITH HEAT GENERATION

BY

SULEIMAN, Aliyu
MTech/SPS/2018/8131

DEPARTMENT OF MATHEMATICS
FEDERAL UNIVERSITY OF TECHNOLOGY MINNA

AUGUST, 2021

ABSTRACT

This thesis considered the analysis of melting heat transfer on magnetohydrodynamics flow of a nanofluid in a porous medium with heat generation and second order slip. The work considered two separate cases with the first case being the classical nanofluid with magnetic, porosity, heat generation and viscous dissipation and the second case introduce melting parameter and second order slip parameter, in addition to the first case. Similarity transformations are introduced to reduce the equations that govern the flow to a system of coupled nonlinear ordinary differential equations. The problems are solved using the Adomian decomposition method. The results obtained for skin frictions $-f''(0)$ are compared with the existing literatures and a good agreement is established. Graphical analysis is done to study the implication of emerging physical parameters such as Inverse Darcy number, Magnetic parameter, Eckert number, Prandtl number, Schmidt number, Melting parameter. The first order slip is taken to be $\delta = 1$ while the second order is $\gamma = -1$ throughout the work. The Inverse Darcy number (Da^{-1} =1, 2, 4), Prandtl number (P_r =0.4, 0.3, 0.1), Schmidt number (S_C =0.3, 0.2, 0.1) are seen as reduction agents of the fluid velocity, fluid temperature and concentration profile respectively. While the Melting parameter (*Me* =0.3, 0.2, 0.1), Eckert number (Ec =0.3, 0.2, 0.1) and Brownian motion (N_b =0.2, 0.4, 0.6) are found to enhance the fluid velocity, fluid temperature and concentration profile respectively.

TABLE OF CONTENTS

LIST OF TABLES

LIST OF FIGURES

Abbreviation, Glossaries and Symbols

u and v	Fluid distances along x and y respectively
P	Fluid pressure
M	Magnetic parameter
Me	Melting parameter
$D^{-1}a$	Inverse Darcy number
ρ_f	Density of base fluid
t	Time
T	Fluid temperature
C	Nanofraction
T_f	Convection fluid temperature
T_m	Temperature at melting surface
T_w	Temperature at wall
T_∞	Temperature at far away from the wall
C_w	Nanoparticles concentration
C_∞	Nanoparticles concentration at far away from the wall
α	Momentum accommodation coefficient
υ	Kinematic viscosity

ψ	Dimensionless stream function
k^*	Thermal conductivity
h^*	Convective heat transfer coefficient
k	Permeability
σ	Electrical conductivity
K_T	Thermal diffusion ratio
φ	Porosity
h^*	Convective heat transfer coefficient
B_0	External magnetic field
Q	Heat generation
C_p	Specific heat capacity at constant pressure
D_B	Brownian Diffusion coefficient
D_T	Thermopheric diffusion coefficient
τ	Ratio between the effective heat capacity of the fluid
G	Acceleration due to gravity
δ	First order slip
γ	Second order slip
η	Dimensionless fluid distance

q_r	Radiative heat flux
Gr_T	Thermal Grashof number
Re	Reynold number
Gr_C	Nanofraction Grashof number
f	Dimensionless fluid velocity
θ	Dimensionless fluid temperature
Ra	Radiation
Pr	Prandtl number
S_C	Schmidt number
N_b	Brownian motion
N_t	Thermopheric parameter
ϕ_0	Heat generation parameter
Ec	Eckert number
ADM	Adomian decomposition method

CHAPTER ONE

1.0 INTRODUCTION

1.1 Background to the Study

Boundary layer theory is an important aspect in the study of a continuously stretching surface into a quiescent fluid, a flow scenario that has garnered much attention over several decades. Some of the applications that involve this scenario include hot rolling, paper production, metal spinning, drawing plastic films, glass blowing, continuous casting of metals, and spinning of fibres. In all of these applications, the quality of the final product depends on the rate of heat transfer at the stretching surface, which is greatly influenced by the rate of stretching and the properties of the cooling fluid (Mabood and Mastroberardino, 2015).

Sakiadis (1961) was one of the first researchers to study two dimensional boundary layer flows over a moving surface in a fluid at rest. The results of this study were later extended by Crane (1970) who included an exact analytical solution for the case of a linearly stretching sheet. It is worth mentioning that both of these studies consider a Newtonian fluid in the analysis. Since the pioneering works of Sakiadis and Crane, a large amount of research has been devoted to the stretching sheet problem mentioned above in which various effects such as suction/injection, porosity, magnetic field parameter, variable material properties, thermal radiation, have been included with consideration of either a Newtonian or non-Newtonian fluid. In recent years, research on boundary layer flow and heat transfer involving nanofluids has received increased attention due their growing importance in numerous industrial and biomedical applications.

Nanofluids are fluids in which nanometer-sized solid particles and/or fibers have been suspended in order to enhance the heat transfer characteristics of the base fluid (Choi,

1995). The nanoparticles typically made of metals, oxides, carbides, or carbon nanotubes come in the form of a powder in which the particles have a diameter ranging between 1 and 100 nm. The thermal conductivities of fluids with suspended particles are expected to be higher than that of common fluids for the following reasons (Khanafer *et al*., 2003):

i. The suspended nanoparticles increase the surface area and the heat capacity of the fluid.
ii. The suspended nanoparticles increase the effective (or apparent) thermal conductivity of the fluid.
iii. The interaction and collision among particles, fluid and the flow passage surface are intensified.
iv. The mixing fluctuation and turbulence of the fluid are intensified.
v. The dispersion of nanoparticles flattens the transverse temperature gradient of the fluid.

According to Yusuf *et al.* (2018), Nanofluid is a new kind of heat transfer medium, containing nanoparticles (1–100 nm) which are uniformly and stably distributed in a base fluid. These distributed nanoparticles, generally a metal or metal oxide greatly enhance the thermal conductivity of the nanofluid, increases conduction and convection coefficients, allowing for more heat transfer.

Nanofluids have been considered for applications as advanced heat transfer fluids for decades. However, due to the wide variety and the complexity of the nanofluid systems, no agreement has been achieved on the magnitude of potential benefits of using nanofluids for heat transfer applications (Yusuf *et al.,* 2019).

1.2 Statement of the Research Problem

Mabood and Mastroberardino (2015) investigated the effects of viscous dissipation and second order slip on MHD boundary layer flow of an incompressible, electrically conducting water-based nanofluid over a stretching sheet. The governing momentum boundary layer and thermal boundary layer equations with the boundary conditions are transformed into a system of nonlinear ordinary differential equations which are then solved numerically by using the Runge–Kutta–Fehlberg method. The effects of the flow parameters on the velocity, temperature, nanoparticle concentration, shearing stress, rate of heat transfer, and rate of mass transfer are analyzed, and illustrations are provided by the inclusion of figures and tables for various values of different parameters.

However, the researchers did not put into consideration the porosity of the medium and the effects of heat generation on the flow. The solutions obtained were not at all points but mesh points.

1.3 Justification of the Study

The failure in the ordinary heat transfer fluid to meet up with today's industrial cooling rate, has resulted into the development of high thermal conductivity fluid, such as nanofluid. Throughout any industrial facility, heat must be added, removed, or moved from one process stream to another and it has become a major task for industrial necessity. These processes provide a source for energy recovery and process fluid heating/cooling (Yusuf *et al.,* 2018).

To the best of the researchers' knowledge, the analysis of melting heat transfer on magneto hydrodynamics flow of a nanofluid in a porous medium with heat generation and second order slip has not been attempted before.

1.4 Aim and Objectives of the Study

1.4.1 Aim of the study

The aim of this study is to carry out the analysis of heat transfer on flow of a nanofluid in a porous medium with heat generation.

1.4.2 Objectives of the study

The objectives of this present study are to:-

i. Transform the Partial differential equation (PDE) formulated to non-linear ordinary differential equations (ODE) using the similarity equations.

ii. Solve the set of transformed nonlinear, coupled, ordinary differential equations (ODE) using the Adomian Decomposition Method (ADM).

iii. Present results for validation with existing methods in the literature.

iv. To draw the graphs from the solution obtain for analysis.

v. Study the effects of the various dimensionless parameters that appears in the solutions.

1.5 Scope and Limitation of the Study

The problems formulated are presented in their rectangular coordinate system. An appropriate similarity transformation is employed to transform the partial differential equations to non-linear coupled ordinary differential equations. The nonlinear coupled ordinary differential equations derived, correspond to velocity, temperature, and nanoparticle concentration equations. These equations are solved using Adomian Decomposition Method. The effect of various parameters that appears are analyzed with the help of graphs. This work is limited to steady parts of an incompressible nanofluid dynamics.

1.6 Definition of Terms

Fluid: A substance which deforms continuously when shear stress is applied to it no matter how small, such as liquid or gas which can flow, has no fixed shape and offers little resistance to an external stress.

Prandtl number: the relationship between the thickness of two boundary layers at a given point along the plate depend on the dimensionless prandtl number which is the ratio of the momentum diffusivity ν or $\frac{\mu}{\rho}$ to the thermal diffusivity $\propto$ or $\frac{k}{\rho Cp}$.

Boundary Layers:- boundary layer is defined as that part of moving fluid in which the fluid motion is influenced by the presence of a solid boundary. As a specific example of boundary layer formation, consider the flow of fluid parallel with a thin plate, when a fluid flows at high Reynolds number past a body, the viscous effects may be neglected everywhere except in a thin region in the vicinity of the walls . This region is termed as the boundary layer.

Magnetohydrodynamics: Is the study of magnetic properties and behavior of electrically conducting fluids.

Compressible fluid: change in density of fluid with time

$$\frac{\Delta\rho}{\Delta t} \neq 0 \qquad (1.1)$$

Incompressible flow: fluid motion with negligible changes in density ρ

$$\frac{\Delta\rho}{\Delta t} = 0 \qquad (1.2)$$

Skin Friction: Is the contact between the moving fluid and solid body.

CHAPTER TWO

2.0 LITERATURE REVIEW

2.1 Reviews on Fluid Dynamics

Recent investigations of boundary layer flow and heat transfer have included the consideration of nanofluids in order to enhance the thermal conductivity (Sheikholeslami and Ganji, 2015). Khan and Pop (2010) investigated boundary layer flow of a nanofluid over a stretching sheet, a work which was then extended by Makinde and Aziz (2012) who considered the effects of convective surface boundary conditions. Rana and Bhargava (2012) performed a similar analysis for a nonlinearly stretching sheet using finite difference and finite element methods. Gbadeyan *et al.* (2011) extended the work of Makinde and Aziz (2012) by including the effects of a magnetic field and thermal radiation. Mabood *et al.* (2015) provided a numerical study of MHD boundary layer flow with viscous dissipation over a nonlinearly stretching sheet and compared the results with those of previous work.

The heat transfer characteristics of a nanofluid depend on the size, volume fraction, shape and thermal properties of nanoparticles as well as the base fluid properties. Generally speaking, numerical simulation of the velocity field, the temperature field and the heat transfer rate of nanofluids can be performed using either a single-phase approach Sheikholeslami et *al*. (2014) or a two-phase approach (Sheikholeslami and Ganji, 2015). The former assumes that the base fluid and the nanoparticles are in thermal equilibrium, and thus, move with the same velocity. The latter considers the notion that slip velocity between the base fluid and the nanoparticles may not be zero, in which case relevant slip mechanisms between solid and liquid phases such as Brownian diffusion and thermophoresis may be included in the model.

The no-slip condition at the surface of the sheet is a well-known assumption in fluid mechanics that has been a basis for much of the theory that has been developed over the last century. However, there are numerous situations in which the no-slip condition leads to erroneous results, particularly when one is considering non-Newtonian fluids or nanofluids. For such fluids, the motion is still governed by first principles, but the usual no-slip condition at the boundary is replaced by a partial slip condition in which the tangential components of the velocity and the stress are nonzero at the boundary. The fluid flow in many applications of micro/nano systems such as hard disk drive, micro pumps, micro-valves and micro-nozzles are characterized by slip flow at wall. One of the first studies to discuss a partial slip boundary condition over a stretching sheet was conducted by Yoshimura and Prudhomme (1988). A later study by Andersson (2002) provided a closed form solution of the governing equations for magnetohydrodynamic flow over a stretching sheet. Since then, numerous researchers have incorporated a partial slip condition whenever it was deemed appropriate.

The Knudsen number a dimensionless number defined as the ratio of the molecular mean free path length to a representative physical length scale—is often used as a basis to determine when the no slip condition is no longer appropriate. In regard to the applicability of partial slip, the first-order model deteriorates for Knudsen number greater than, and therefore, a number of researchers have proposed second-order slip flow model. Wu (2008) has proposed a second-order slip flow model for the flow of rarefied fluid along the surface based on numerical simulation of linearized Boltzmann equation. Zhang *et al*. (2008) validated the Navier–Stokes equation with second-order slip in a transition region by using the homotopy analysis method. Fang *et al.* (2010) studied the flow of a viscous fluid over a shrinking sheet with second-order slip.

Nandeppanavar *et al.* (2012) considered second-order slip flow and heat transfer over a stretching sheet with a non-linear Navier boundary condition.

In real world, most of the fluids such as water, kerosene oil, ethylene, glycol, and others are poor conductors of heat due to their lower values of thermal conductivity. To cope up with this problem and to enhance the thermal conductivity or other thermal properties of these fluids, a newly developed technique is used which includes, addition of nano-sized particles of good conductors such as copper, aluminum, titanium, iron and other oxides to the fluids. Choi (1995) was the first one to come up with this idea and also showed that the thermal conductivity of conventional fluids can be doubled by adding nano particles to base fluids that also incorporate other thermal properties. These enhancements can be used practically in electronic cooling, heat exchangers, double plane windows. Buongiorno (2006) presented a more comprehensive model for the nanotechnology based fluids that unveils the thermal properties superior to base fluids. He discussed all the convective properties of nanofluids by developing a more general model. After these developments in nanofluids, Khan and Pop (2010) were the first ones to study boundary layer flow over a stretching sheet by using the model of Nield and Kuznetsov (2009). Mustafa *et al.* (2011) presented first study on stagnation point flow of a nanofluid. They presented both Brownian motion and thermophoresis effects on transport equations by reducing them to a nonlinear boundary value problem. One can easily find enough literature on nano fluid flows, however some of the studies are reported in Nadeem and Haq (2013) and references therein. Study of electrically conducting fluids hold importance due to applications in modern metallurgy and metal working processes. Magnetic nanofluids are used to regulate the flow and heat transfer by controlling the fluid velocity. Mahapatra (2002) studied MHD stagnation point flow over a stretching sheet using numerical simulations. MHD stagnation point flow for

nanofluid was presented by Ibrahim *et al.* (2013) employing fourth order Runge-Kutta technique. Some others studies regarding magneto-nanofluids are presented in Nadeem and Lee (2012) and references therein. In all presented studies, Soret and Dufour effects were neglected. It is a well-known fact that the temperature and concentration gradients present mass and energy fluxes, respectively. Concentration gradients result in Dufour effect (diffusion-thermo) while Soret effect (thermal-diffusion) is due to temperature gradients. Such effects play a significant role when there are density differences in the flow. For the flows of mixture of gases with light molecular weights and moderate weights, Soret and Dufour effects cannot be neglected. Thermo-diffusion effects on the flow over a stretching sheet are examined by Awad *et al.* (2013).

Ramachandra *et al.* (1988) have investigated the mixed convection flow in the stagnation flow region of a vertical plate. The steady stagnation-point flow towards a permeable vertical surface was investigated by Ishak *et al.* (2008). Li et al. (2011) introduced an analysis of the steady mixed convection flow of a viscoelastic fluid stagnating orthogonally on a heated or cooled vertical flat plate. Makinde (2012) examined the hydromagnetic mixed convection stagnation-point flow towards a vertical plate embedded in a highly porous medium with radiation and internal heat generation. Mabood and Khan (2014) introduced an accurate analytic solution (series solution) for MHD stagnation-point flow in a porous medium for different values of the Prandtl number and the suction/injection parameter. An unsteady boundary layer plays important roles in many engineering problems like a start-up process and a periodic fluid motion. An unsteady boundary layer has different behaviors due to extra time-dependent terms, which will influence the fluid motion pattern and the boundary-layer separation. Kumari *et al.* (1992) have studied the unsteady mixed convection flow of an electrically conducting fluid at the stagnation point of a two-dimensional body and an

axisymmetric body in the presence of an applied magnetic field. Seshadri *et al.* (2002) studied the unsteady mixed convection in the stagnation-point flow on a heated vertical plate where the unsteadiness is caused by the impulsive motion of the free stream velocity and by sudden increase in the surface temperature (heat flux). Hassanien *et al.* (2004) analyzed the problem of unsteady free convection flow in the stagnation-point region of a rotating sphere embedded in a porous medium. The unsteady flow and heat transfer of a viscous fluid in the stagnation region of a three-dimensional body embedded in a porous medium was investigated by Hassanien *et al.* (2006). Hassanien and Al-Arabi (2008) studied the problem of thermal radiation and variable viscosity effects on unsteady mixed convection flow in the stagnation region on a vertical surface embedded in a porous medium with surface heat flux. Fang *et al.* (2011) investigated the boundary layers of an unsteady incompressible stagnation-point flow with mass transfer. Shateyi and Marewo (2014) have numerically investigated the problem of unsteady MHD flow near a stagnation point of a two-dimensional porous body with heat and mass transfer in the presence of thermal radiation and chemical reaction. Rosali *et al.* (2014) discussed the effect of unsteadiness on mixed convection boundary-layer stagnation-point flow over a vertical flat surface embedded in a porous medium.

Vasu and Manish (2015) studied the problem of two-dimensional transient hydrodynamic boundary-layer flow of an incompressible Newtonian nanofluid past a cone and plate with constant boundary conditions. Gireesha *et al.* (2015) introduced a numerical solution for hydromagnetic boundary-layer flow and heat transfer past a stretching surface embedded in a non-Darcy porous medium with fluid-particle suspension. The unsteady forced convective boundary-layer flow of an incompressible non-Newtonian nanofluid over a stretching sheet when the sheet is stretched in its own plane is investigated by Gorla and Vasu (2016). Gorla *et al.* (2016) investigated the

transient mixed convective boundary-layer flow of an incompressible non-Newtonian quiescent nanofluid adjacent to a vertical stretching surface. The unsteady flow and heat transfer of a nanofluid over a contracting cylinder was studied by Zaimi *et al.* (2014). Srinivasacharya and Surender (2014) studied the effects of thermal and mass stratification on natural convection boundary-layer flow over a vertical plate embedded in a porous medium saturated by a nanofluid.

During the past decade, the study of nanofluids has attracted enormous interest from researchers due to their exceptional applications to electronics, automotive, communication, computing technologies, optical devices, lasers, high-power X-rays, scientific measurement, material processing, medicine, and material synthesis, where efficient heat dissipation is necessary. Nanobiotechnology is also a fast-developing field of research and application in many domains, such as in medicine, pharmacy, cosmetics and agro-industry. Nanofluids are prepared by dispersing solid nanoparticles in base fluids such as water, oil, ethylene glycol, or others. According to Yacob *et al.* (2011), nanofluids are produced by dispersing the nanometer-scale solid particles into base liquids with low thermal conductivity such as water and ethylene glycol. Nanoparticles are usually made of metal, metal oxide, carbide, nitride, and even immiscible nanoscale liquid droplets. Congedo *et al.* (2009) compared different models of nanofluids (regarded as a single phase) to investigate the density, specific heat, viscosity, and thermal conductivity, and discussed the water–Al2O3 nanofluid in detail by using CFD. Hamad *et al.* (2011) introduced a one-parameter group to represent similarity reductions for the problem of magnetic field effects on free-convective nanofluid flow past a semi infinite vertical flat plate following a nanofluid model proposed by Buongiorno (2006). Hady *et al.* (2012a) studied the radiation effect on viscous flow of a nanofluid and heat transfer over a nonlinearly stretching sheet with variable wall temperature. Also, Hady

et al. (2012b) studied the problem of natural convection boundary-layer flow past a porous plate embedded in a porous medium saturated with a nanofluid using Buongiorno's model. Further, Abu-Nada and Chamkha (2010) presented the natural convection heat transfer characteristics in a differentially heated enclosure filled with CuO–ethylene glycol (EG)–water nanofluids for different variable thermal conductivity and variable viscosity models. Rudraswamy and Gireesha (2015) studied the problem of flow and heat transfer of a nanofluid over an exponentially stretching sheet by considering the effect of chemical reaction and thermal radiation. Besthapu and Bandari (2015) presented a study on the mixed convection MHD flow of a Casson nanofluid over a nonlinear permeable stretching sheet with viscous dissipation. A numerical solution of the natural convection flow of a two-phase dusty nanofluid along a vertical wavy frustum of a cone is discussed by Siddiqa *et al.* (2016a). The bioconvection flow with heat and mass transfer of a water-based nanofluid containing gyrotactic microorganisms over a vertical wavy surface is studied by Siddiqa *et al*. (2016b). Kameswaran *et al.* (2016) studied convective heat transfer in the influence of nonlinear Boussinesq approximation, thermal stratification, and convective boundary conditions on non-Darcy nanofluid flow over a vertical wavy surface.

The effects of radiation on unsteady free convection flow and heat transfer problem have become more important industrially. At high operating temperature, radiation effect can be quite significant. Many processes in engineering areas occur at high temperature and knowledge of radiation heat transfer becomes very important for design of reliable equipment, nuclear plants, gas turbines and various propulsion devices or aircraft, missiles, satellites and space vehicles. Based on these applications, Cogley *et al.* (1968) showed that in the optically thin limit, the fluid does not absorb its own emitted radiation but the fluid does absorb radiation emitted by the boundaries. Hossain and

Takhar (1996) have considered the radiation effects on mixed convection boundary layer flow of an optically dense viscous incompressible fluid along a vertical plate with uniform surface temperature. Makinde (2005) examined the transient free convection interaction with thermal radiation of an absorbing emitting fluid along moving vertical permeable plate. Satter and Hamid (1996) investigated the unsteady free convection interaction with thermal radiation of an absorbing emitting plate.

Flow of a nanofluid in a boundary layer in an inclined moving sheet at angle Θ is considered analytically by Yusuf *et al.* (2019), the Mathematical formulation consists of the Magnetic parameter, thermophoresis, and Brownian motion. Solutions to momentum, temperature and concentration distribution depends on some parameters. The non-linear coupled Differential equations were solved using the improved Adomian decomposition method and a good agreement was established with the numerical method (Shooting technique).

Abdullah *et al.* (2018) studies the effects of Brownian motion and thermophoresis on unsteady mixed convection flow near the stagnation-point region of a heated vertical plate embedded in a porous medium saturated by a nanofluid. The plate is maintained at a variable wall temperature and nanoparticle volume fraction. The presence of a solid matrix, which exerts first and second resistance parameters, is considered in the study. A suitable coordinate transformation is introduced and the resulting governing equations are transformed and then solved numerically using the local non-similarity method and the Runge-Kutta shooting quadrature. The effects of various governing parameters on the flow and heat and mass transfer on the dimensionless velocity, temperature, and nanoparticle volume fraction profiles as well as the skin-friction coefficient, Nusselt number, and the Sherwood number are displayed graphically and discussed to illustrate interesting features of the solutions. The results indicate that as the values of the

thermophoresis and Brownian motion parameters increase, the local skin-friction coefficient increases whereas the Nusselt number decreases.

Moreover, the Sherwood number increases as the thermophoresis parameter increases, and decreases as the Brownian motion parameter increases. On the other hand, the unsteadiness parameter and the resistance parameters enhance the local skin-friction coefficient, local Nusselt number, and the local Sherwood number.

2.2 Adomian Decomposition Method (ADM)

Begin with an equation $Fu(t) = g(t)$, where F represents a general nonlinear ordinary differential operator involving both linear and nonlinear terms. The linear term is decomposed into $L + R$, where L is easily invertible and R is the remainder of the linear operator. For convenience, L may be taken as the highest order derivative which avoids difficult integrations which result when complicated Green's functions are involved Adomian (1994). Thus the equation may be written as:

$$Lu + Ru + Nu = g \tag{2.1}$$

where Nu represents the nonlinear terms. Solving for Lu,

$$Lu = g - Ru - Nu \tag{2.2}$$

Because L is invertible, an equivalent expression is

$$L^{-1}Lu = L^{-1}g + L^{-1}Ru - L^{-1}Nu \tag{2.3}$$

If this corresponds to an initial-value problem, the integral operator L^{-1} may be regarded as definite integrals from t_0 to t. If L is a second-order operator, L^{-1} is a twofold integration operator and $L^{-1}Lu = u - u(t_0) - (t - t_0)u'(t_0)$. For boundary value problems (and, if desired, for initial-value problems as well), indefinite integrations are used and the constants are evaluated from the given conditions.

$$u = A + Bt + L^{-1}g + L^{-1}Ru - L^{-1}Nu \tag{2.4}$$

The nonlinear term Nu will be equated to $\sum_{n=0}^{\infty} A_n$, where the A_n , are special polynomials to be discussed, and u will be decomposed into $\sum_{n=0}^{\infty} u_n$, with u_0 identified as $A + Bt + L^{-1}g$

$$\sum_{n=0}^{\infty} u_n = u_0 - L^{-1}R\sum_{n=0}^{\infty} u_n - L^{-1}\sum_{n=0}^{\infty} A_n \tag{2.5}$$

Consequently, we can write to

$$\left.\begin{aligned} u_1 &= -L^{-1}Ru_0 - L^{-1}A_0 \\ u_2 &= -L^{-1}Ru_1 - L^{-1}A_0 \\ &\vdots \\ u_{n+1} &= -L^{-1}Ru_n - L^{-1}A_n \end{aligned}\right\}$$

The polynomials A_n, are generated for each nonlinearity so that A_0, depends only on u_0, A_1 , depends only on u_0 ,and u_1 , A_2 , depends on u_0 , u_1 , u_2 , etc. All of the u_n , components are calculable, and $u = \sum_{n=0}^{\infty} u_n$. If the series converges, the n -term partial sum $\phi_n = \sum_{i=0}^{n-1} u_i$ will be the approximate solution since $\lim_{n\to\infty} \phi_n = \sum_{i=0}^{\infty} u_i = u$ by definition.

It is important to emphasize that the A_n can be calculated for complicated nonlinearities of the form $f\left(u,\ u^{/},...\right)$ or $f\left(g\left(u\right)\right)$.

Mabood and Mastroberardino (2015) Consider a two dimensional, incompressible viscous flow of a water-based nanofluid past over a stretching sheet. The sheet is extended with velocity $u_w = ax$ with fixed origin location, where a is a constant and x is the coordinate measured along the stretching surface. The nanofluid flows at $y = 0$, where y is the coordinate normal to the surface. The fluid is electrically conducted due

to a constant magnetic field normal to the stretching sheet. The magnetic Reynolds number is assumed small and so, the induced magnetic field can be considered to be negligible. It is assumed that the temperature of the melting surface is *Tm* and the temperature in free-stream is $T\infty$, where *($T\infty$ > Tm)*, the nanoparticle fraction *Cw* is assumed constant at the stretching surface. When *y* tends to infinity, the ambient value of nanoparticle fraction is denoted by $C\infty$. The governing equations of momentum, thermal energy and nanoparticles equations are given by:

$$\frac{\partial u}{\partial x}+\frac{\partial v}{\partial y}=0 \tag{2.6}$$

$$\left(u\frac{\partial u}{\partial x}+v\frac{\partial u}{\partial y}\right)=\upsilon\left(\frac{\partial^2 u}{\partial x^2}+\frac{\partial^2 u}{\partial y^2}\right)-\frac{\sigma B_0^2}{\rho_f}u \tag{2.7}$$

$$\left(u\frac{\partial T}{\partial x}+v\frac{\partial T}{\partial y}\right)=\alpha\left(\frac{\partial^2 T}{\partial x^2}+\frac{\partial^2 T}{\partial y^2}\right)+\tau\left[D_B\left(\frac{\partial C\partial T}{\partial x\partial x}+\frac{\partial C\partial T}{\partial y\partial y}\right)+\frac{D_T}{T_\infty}\left(\frac{\partial T}{\partial x}+\frac{\partial T}{\partial y}\right)^2\right]+$$

$$\frac{\upsilon}{c_p}\left(\frac{\partial u}{\partial y}\right)^2 \tag{2.8}$$

$$\left(u\frac{\partial C}{\partial x}+v\frac{\partial C}{\partial y}\right)=D_B\left(\frac{\partial^2 C}{\partial x^2}+\frac{\partial^2 C}{\partial y^2}\right)+\frac{D_T}{T_\infty}\left(\frac{\partial^2 T}{\partial x^2}+\frac{\partial^2 T}{\partial y^2}\right) \tag{2.9}$$

Subject to the boundary condition:

$$\left.\begin{array}{l} y=0: u=u_w+u_{slip},\ \ T=T_m,\ \mathrm{k}\left(\dfrac{\partial T}{\partial y}\right)=\rho\left(\lambda+c_s\left(T_m-T_0\right)\right)\mathrm{v}\left(x,0\right),\mathrm{C}=\mathrm{C}_w \\ \mathrm{y}\to\infty: u=0,\ T=T_\infty,\mathrm{C}=\mathrm{C}_\infty \end{array}\right\} \tag{2.10}$$

The present work extends Mabood and Mastroberardino (2015) by in-cooperating the porosity of the medium and heat generation. The analysis is also carried out analytically using the Adomian decomposition method. From the available literatures, this innovation is new.

CHAPTER THREE

3.0 MATERIALS AND METHODS

3.1 Problem Formulation

Considering two dimensional, incompressible viscous flow of a water-based nanofluid past over a stretching sheet. The sheet stretches with a velocity *ax*, where *a* is a constant and *x* is the coordinate measured along the stretching surface. The fluid flow at *y=0,* where *y* is the coordinate normal to the surface. The temperature of the melting surface is taken as T_m and at larger values, it is taken as T_∞ with $T_\infty \succ T_m$. The nanoparticle concentration C_w is assumed constant on the stretching surface and C_∞ at larger values of *y*. Following the formulation in Mabood and Mastroberardino (2015) in a porous medium with heat generation, the governing equations of continuity, momentum, temperature, and nanoparticle concentration are written as:

$$\frac{\partial u}{\partial x}+\frac{\partial v}{\partial y}=0 \tag{3.1}$$

$$\left(u\frac{\partial u}{\partial x}+v\frac{\partial u}{\partial y}\right)=\upsilon\left(\frac{\partial^2 u}{\partial x^2}+\frac{\partial^2 u}{\partial y^2}\right)-\frac{\sigma B_0^2}{\rho_f}u-\frac{\upsilon\varphi}{k}u \tag{3.2}$$

$$\left(u\frac{\partial T}{\partial x}+v\frac{\partial T}{\partial y}\right)=\alpha\left(\frac{\partial^2 T}{\partial x^2}+\frac{\partial^2 T}{\partial y^2}\right)+\tau\left[D_B\left(\frac{\partial C\partial T}{\partial x\partial x}+\frac{\partial C\partial T}{\partial y\partial y}\right)+\frac{D_T}{T_\infty}\left(\frac{\partial T}{\partial x}+\frac{\partial T}{\partial y}\right)^2\right]+$$
$$\frac{\upsilon}{c_p}\left(\frac{\partial u}{\partial y}\right)^2+\frac{Q}{\rho c_p}\left(T-T_m\right) \tag{3.3}$$

$$\left(u\frac{\partial C}{\partial x}+v\frac{\partial C}{\partial y}\right)=D_B\left(\frac{\partial^2 C}{\partial x^2}+\frac{\partial^2 C}{\partial y^2}\right)+\frac{D_T}{T_\infty}\left(\frac{\partial^2 T}{\partial x^2}+\frac{\partial^2 T}{\partial y^2}\right) \tag{3.4}$$

Subject to the boundary condition:

$$\left.\begin{array}{l} y=0: u=u_w+u_{slip},\ \ T=T_m,\ \mathrm{k}\left(\dfrac{\partial T}{\partial y}\right)=\rho\left(\lambda+c_s\left(T_m-T_0\right)\right)\mathrm{v}\left(x,0\right),\mathrm{C}=\mathrm{C}_w \\ \mathrm{y}\to\infty: u=0,\ T=T_\infty,\mathrm{C}=\mathrm{C}_\infty \end{array}\right\} \tag{3.5}$$

According to Nanndepparavar *et al.* (2012), the velocity of slip is given by:

$$u_{slip}=A\frac{\partial u}{\partial y}+B\frac{\partial^2 u}{\partial y^2} \tag{3.6}$$

Where

$$A=\frac{2}{3}\left(\frac{3-\alpha l^3}{\alpha}-\frac{3}{2}\frac{1-l^2}{k_n}\right)\lambda,\quad B=\frac{1}{4}\left(l^4+\frac{2}{k_n^2}\left(1-l^2\right)\right)\lambda^2,\ \ l=\min\left(\frac{1}{k_n},1\right),$$

α is the momentum accomodation coefficient with $0\le\alpha\le 1$ and λ is the molecular mean free path.

In order to reduce the PDEs into ODEs, the following similarity variables are defined as follows:

$$\eta=\sqrt{\frac{a}{\upsilon}}y,\ \ u=axf'\left(\eta\right),\ \ v=-\sqrt{a\upsilon}f\left(\eta\right),\theta=\frac{T-T_m}{T_\infty-T_m},\phi=\frac{C-C_\infty}{C_w-C_\infty} \tag{3.7}$$

From the similarity equation in (3.7),

$$
\left.
\begin{aligned}
&\eta = \sqrt{\frac{a}{\upsilon}}y, u = axf^{/}, v = -\sqrt{a\upsilon}f(\eta)\\
&\frac{\partial u}{\partial y} = \frac{\partial u}{\partial \eta}\frac{\partial \eta}{\partial y} = axf^{//}\sqrt{\frac{a}{\upsilon}}\ ,\ \frac{\partial u}{\partial x} = af^{/}\\
&\frac{\partial^2 u}{\partial y^2} = \frac{\partial}{\partial y}\left(axf^{//}\sqrt{\frac{a}{\upsilon}}\right) = \frac{\partial \eta}{\partial y}\frac{\partial}{\partial \eta}\left(axf^{//}\sqrt{\frac{a}{\upsilon}}\right) = \frac{a^2 x}{\upsilon}f^{///}\\
&u\frac{\partial u}{\partial x} = axf^{/}af^{/} = a^2 xf^{/2}\\
&v\frac{\partial u}{\partial y} = -\sqrt{a\upsilon}f(\eta)a\sqrt{\frac{a}{\upsilon}}xf^{//} = -a^2 xff^{//}\\
&T = T_m + (T_\infty - T_m)\theta(\eta), \mathrm{C} = C_\infty + (C_W - C_\infty)\phi(\eta)\\
&\frac{\partial T}{\partial x} = 0,\ \frac{\partial T}{\partial y} = (T_\infty - T_m)\frac{\partial \eta}{\partial y}\frac{\partial}{\partial \eta}\theta(\eta) = (T_\infty - T_m)\sqrt{\frac{a}{\upsilon}}\theta^{/}\\
&\frac{\partial C}{\partial x} = 0,\ \frac{\partial C}{\partial y} = (C_W - C_\infty)\frac{\partial \eta}{\partial y}\frac{\partial}{\partial \eta}\phi(\eta) = (C_W - C_\infty)\sqrt{\frac{a}{\upsilon}}\phi^{/}\\
&\frac{\partial^2 T}{\partial y^2} = \frac{\partial}{\partial y}\left((T_\infty - T_m)\sqrt{\frac{a}{\upsilon}}\theta^{/}\right) = \frac{\partial \eta}{\partial y}\frac{\partial}{\partial \eta}\left((T_\infty - T_m)\sqrt{\frac{a}{\upsilon}}\theta^{/}\right) = (T_\infty - T_m)\frac{a}{\upsilon}\theta^{//}\\
&\frac{\partial^2 C}{\partial y^2} = \frac{\partial}{\partial y}\left((C_W - C_\infty)\sqrt{\frac{a}{\upsilon}}\phi^{/}\right) = \frac{\partial \eta}{\partial y}\frac{\partial}{\partial \eta}\left((C_W - C_\infty)\sqrt{\frac{a}{\upsilon}}\phi^{/}\right) = (C_W - C_\infty)\frac{a}{\upsilon}\phi^{//}\\
&v\frac{\partial T}{\partial y} = -\sqrt{a\upsilon}f(\eta)\sqrt{\frac{a}{\upsilon}}(T_\infty - T_m)\theta^{/} = a(T_\infty - T_m)f\theta^{/}\\
&v\frac{\partial C}{\partial y} = -\sqrt{a\upsilon}f(\eta)\sqrt{\frac{a}{\upsilon}}(C_w - C_\infty)\phi^{/} = a(C_w - C_\infty)f\phi^{/}
\end{aligned}
\right\} \qquad (3.8)
$$

Introducing equation (3.8) into (3.1) to (3.5), the equations reduces to

$$
\left.
\begin{aligned}
&f^{///} + ff^{//} - f^{/2} - \left(M + Da^{-1}\right)f^{/} = 0\\
&\theta^{//} + P_r f\theta^{/} + P_r N_b\theta^{/}\phi^{/} + P_r N_t\theta^{/2} + P_r Ecf^{//2} + P_r Q_0\theta = 0\\
&\phi^{//} + S_C f\phi^{/} + \frac{N_t}{N_b}\theta^{//} = 0\\
&f^{/}(0) = 1 + \delta f^{//}(0) + \gamma f^{///}(0),\\
&\theta(0) = 0, \mathrm{Me}\theta^{/}(0) + P_r f(0) = 0, \phi(0) = 1\\
&f^{/}(\infty) = 0, \theta(\infty) = 1, \phi(\infty) = 0
\end{aligned}
\right\} \qquad (3.9)
$$

Where;

$$M=\frac{\sigma B_0^2}{a\rho_f},\ \ Da^{-1}=\frac{\upsilon\varphi}{ak_0},P_r=\frac{\upsilon}{\alpha},\mathrm{N}_b=\frac{\tau D_B\left(C_w-C_\infty\right)}{\upsilon},\mathrm{N}_t=\frac{\tau D_T}{\upsilon T_\infty}\left(T_\infty-T_m\right),\mathrm{Ec}=\frac{a^2x^2\upsilon}{c_p\left(T_\infty-T_m\right)}$$

$$Q_0=\frac{Q}{a\rho c_p},\mathrm{S}_C=\frac{\upsilon}{D_B},Me=\frac{\left(T_\infty-T_m\right)}{\lambda+c_s\left(T_m-T_0\right)},\delta=\mathrm{A}\sqrt{\frac{a}{\upsilon}}\left(\succ 0\right),\text{and }\gamma=\frac{Ba}{\upsilon}\left(\prec 0\right).$$

Are Magnetic parameter, inverse Darcy number, Prandtl number, Brownian motion, thermophoresis parameter, Eckert number, Heat generation, Schmidt number, Melting parameter, first and second order slip parameter respectively.

From equation (3.9), taking $Me=\delta=\gamma=0$ with the assumption that $T_m=T_w\succ T_\infty$, the equations reduces to classical problem of nanofluid flow and heat transfer due to stretching sheet given as:

$$\left.\begin{aligned}
&f'''+ff''-f'^2-\left(M+Da^{-1}\right)f'=0\\
&\theta''+P_rf\theta'+P_rN_b\theta'\phi'+P_rN_t\theta'^2+P_rEcf''^2+P_rQ_0\theta=0\\
&\phi''+S_Cf\phi'+\frac{N_t}{N_b}\theta''=0\\
&f\left(0\right)=0,f'\left(0\right)=1,\theta\left(0\right)=1,\phi\left(0\right)=1\\
&f'\left(\infty\right)=0,\theta\left(\infty\right)=0,\phi\left(\infty\right)=0
\end{aligned}\right\}\qquad(3.10)$$

Let $\frac{d^3}{d\eta^3}=L_1$ and $\frac{d^2}{d\eta^2}=L_2$ and from problem (3.10), we have

$$\left.\begin{aligned}
f'''&=-ff''+f'^2+\left(M+Da^{-1}\right)f'\\
\theta''&=-P_rf\theta'-P_rN_b\theta'\phi'-P_rN_t\theta'^2-P_rE_Cf''-P_rQ_0\theta\\
\phi''&=-S_Cf\phi'-\frac{N_t}{N_b}\theta''
\end{aligned}\right\}\qquad(3.11)$$

Introducing the operators into equations (3.11) we have

$$\left.\begin{aligned} L_1^{-1}L_1\left[f(\eta)\right] &= L_1^{-1}\left[-ff'' + f'^2 + M\left(M + Da^{-1}\right)f'\right] \\ L_2^{-1}L_2\left[\theta(\eta)\right] &= L_2^{-1}\left[-P_r f\theta' - P_r N_b\theta'\phi' - P_r N_t\theta'^2 - P_r E_C f''^2 - P_r Q_0\theta\right] \\ L_2^{-1}L_2\left[\phi(\eta)\right] &= L_2^{-1}\left[-S_C f\phi' - \frac{N_t}{N_b}\theta''\right] \end{aligned}\right\} \tag{3.12}$$

Where $L_1^{-1} = \int\int\int(\bullet)\,d\eta d\eta d\eta$ and $L_2^{-1} = \int\int(\bullet)\,d\eta d\eta$ (3.13)

Introducing the Adomian polynomials into (3.12) we

$$\left.\begin{aligned} &\sum_{n=0}^{\infty} f_n = -L_1^{-1}\sum_{n=0}^{\infty} A_n + L_1^{-1}\sum_{n=0}^{\infty} B_n + \left(M + Da^{-1}\right)L_1^{-1}\sum_{n=0}^{\infty} f_n' \\ &\sum_{n=0}^{\infty}\theta_n = -P_r L_2^{-1}\sum_{n=0}^{\infty} C_n - P_r N_b L_2^{-1}\sum_{n=0}^{\infty} D_n - P_r N_t L_2^{-1}\sum_{n=0}^{\infty} E_n - P_r E_C L_2^{-1}\sum_{n=0}^{\infty} F_n - P_r Q_0 L_2^{-1}\sum_{n=0}^{\infty}\theta_n \\ &\text{have } \sum_{n=0}^{\infty}\phi_n = -S_C L_2^{-1}\sum_{n=0}^{\infty} G_n - \frac{N_t}{N_b}L_2^{-1}\sum_{n=0}^{\infty}\theta_n'' \\ &\textit{where } A_n = f_n f_{n-k}'', B_n = f_n' f_{n-k}', \mathrm{C}_n = f_n\theta_{n-k}', D_n = \theta_n'\phi_{n-k}', \ \mathrm{E}_n = \theta_n'\theta_{n-k}', \mathrm{F}_n = f_n'' f_{n-k}'' \\ &G_n = f_n\phi_{n-k}', \end{aligned}\right\} \tag{3.14}$$

$$
\left.
\begin{aligned}
f_{n+1} &= -L_1^{-1}\sum_{k=0}^{n} f_n f_{n-k}^{//} + L_1^{-1}\sum_{k=0}^{n} f_n^{/} f_{n-k}^{/} + \left(M + Da^{-1}\right) L_1^{-1} f_n^{/} \\
\theta_{n+1} &= -P_r L_2^{-1}\sum_{k=0}^{n} f_n \theta_{n-k}^{/} - P_r N_b L_2^{-1}\sum_{k=0}^{n} \theta_n^{/}\phi_{n-k}^{/} - P_r N_t L_2^{-1}\sum_{k=0}^{n} \theta_n^{/}\theta_{n-k}^{/} \\
&- P_r E_C L_2^{-1}\sum_{k=0}^{n} f_n^{//} f_{n-k}^{//} - P_r Q_0 L_2^{-1}\theta_n^{/} \\
\phi_{n+1} &= -S_C L_2^{-1}\sum_{k=0}^{n} f_n \phi_{n-k}^{/} - \frac{N_t}{N_b} L_2^{-1}\theta_n^{//}
\end{aligned}
\right\} \tag{3.15}
$$

In order to obtain the solution to problem (3.9), the initial guesses for (3.15) are taking as:

$$
\left.
\begin{aligned}
f_0(\eta) &= \eta\left(1 + \delta\alpha_4 + \gamma\alpha_5\right) - \frac{\sqrt{M + Da^{-1}}}{2}\eta^2 - \frac{Me\alpha_6}{P_r} \\
\theta_0(\eta) &= \eta^3\alpha_6 \\
\phi_0(\eta) &= 1 + \eta\alpha_7
\end{aligned}
\right\} \tag{3.16}
$$

Where $\alpha_4 = f^{//}(0)$, $\alpha_5 = f^{///}(0)$ and $\alpha_6 = \theta^{/}(0)$

Using maple18 to evaluate the integrals we have the final solutions as:

$$
\left.
\begin{aligned}
f(\eta) &= \sum_{n=0}^{3} f_n(\eta) \\
\theta(\eta) &= \sum_{n=0}^{3} \theta_n(\eta) \\
\phi(\eta) &= \sum_{n=0}^{3} \phi_n(\eta)
\end{aligned}
\right\} \tag{3.17}
$$

Corresponding to: Appendix A

In order to obtain the solution to problem (3.10), the initial guesses for (3.15) are taking as:

$$\left.\begin{aligned} f_0(\eta) &= \eta - \frac{\alpha_1\left(\sqrt{M + Da^{-1}}\right)\eta^2}{2} \\ \theta_0(\eta) &= 1 + \eta\alpha_2 \\ \phi_0(\eta) &= 1 + \eta\alpha_3 \end{aligned}\right\} \tag{3.18}$$

Using maple18 to evaluate the integrals we have the final solutions as:

$$\left.\begin{aligned} f(\eta) &= \sum_{n=0}^{3} f_n(\eta) \\ \theta(\eta) &= \sum_{n=0}^{3} \theta_n(\eta) \\ \phi(\eta) &= \sum_{n=0}^{3} \phi_n(\eta) \end{aligned}\right\} \tag{3.19}$$

Corresponding to: Appendix B

CHAPTER FOUR

4.0 RESULTS AND DISCUSSION

4.1 Results

In this chapter, comparison of previous works in the literature with the present study is presented in the Table 4.1 below. Also the graphs showing the effects of various physical parameters that occur in the solutions are presented and discussed.

Table 4.1: Comparison of values of skin friction with existing solutions for $Me = \delta = \gamma = 0$

M	Present Results	Mabood and Mastroberardino (2015)	Xu and Lee (2013)
0	———	-1.000008	
1	1.3305610	1.4142135	1.41421
5	2.384890	2.4494897	2.4494
10	3.267599	3.3166247	3.3166
50	7.118200	7.1414284	7.1414
100	10.03333	10.049875	10.0498
500	22.375586	22.383029	22.38302
1000	31.633317	31.638584	———

4.2 Presentation of Graphical Results for the Solution of Classical Problem with Melting and Second order Slip Parameters.

The graphical results for the problem of magnetic effect, Darcy number, slip parameter and melting parameter are presented in this section. Throughout, the first order slip is kept at 1 and second order slip is kept at -1 and while a parameter is varied, orders are

kept constant.

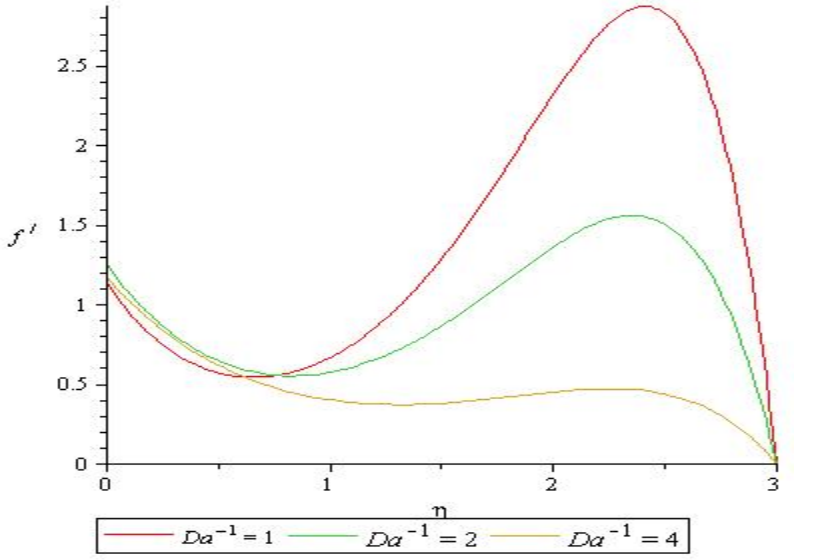

Figure 4.1: Variation of inverse Darcy number on velocity profile with slip

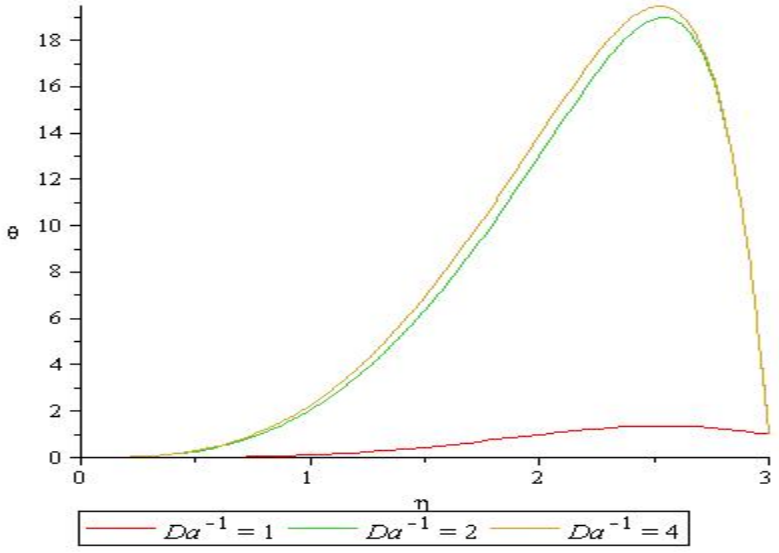

Figure 4.2: Variation of inverse Darcy number on temperature profile with slip

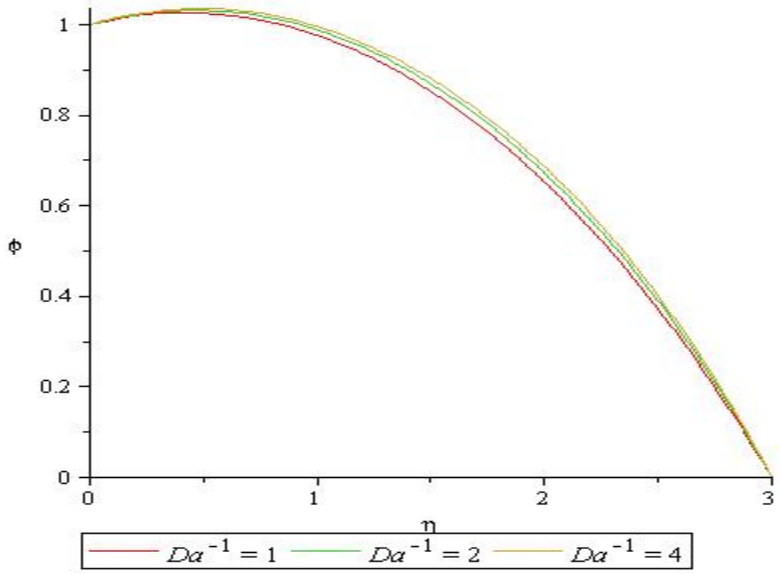

Figure 4.3: Variation of inverse Darcy number on concentration profile with slip

Figures 4.1 to 4.3 presents the variation of inverse Darcy parameter on velocity profile, temperature and concentration profiles respectively. It is observe that as the inverse Darcy number increases, the fluid velocity reduces while temperature and concentration increases. The temperature is seen to be zero on the melting surface and started rising after some distance.

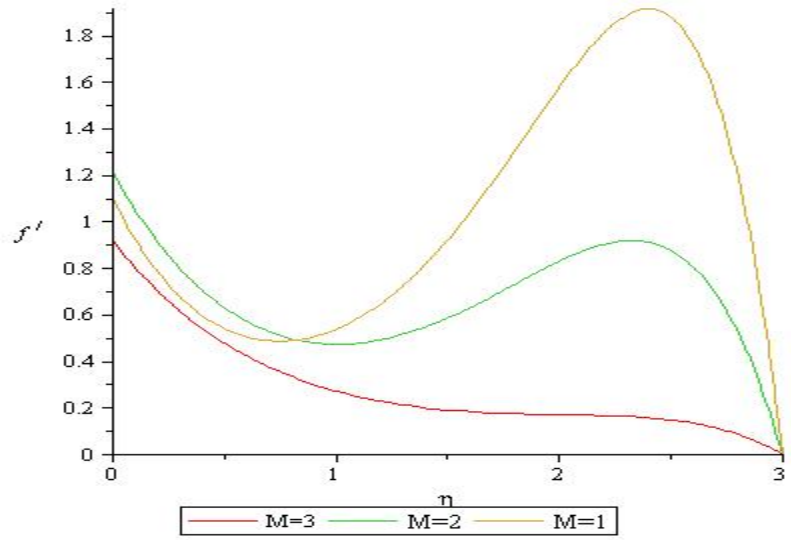

Figure 4.4: Variation of magnetic parameter on velocity profile with slip

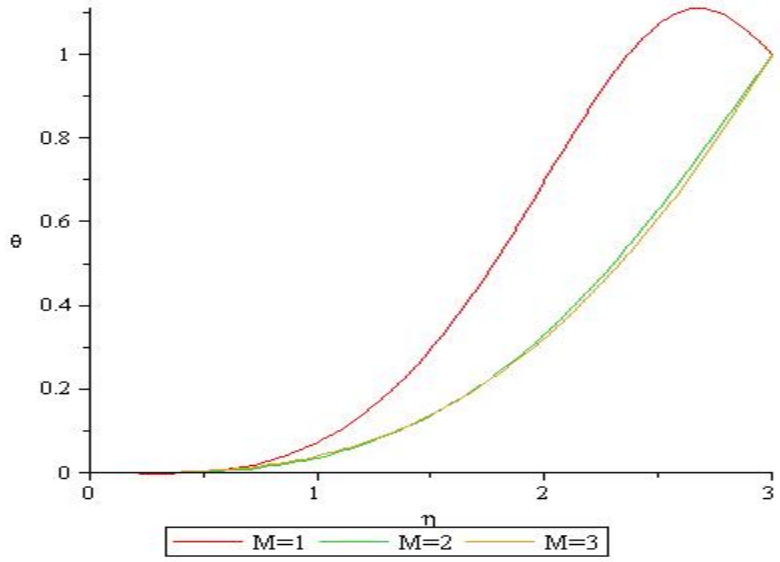

Figure 4.5: Variation of magnetic parameter on temperature profile with slip

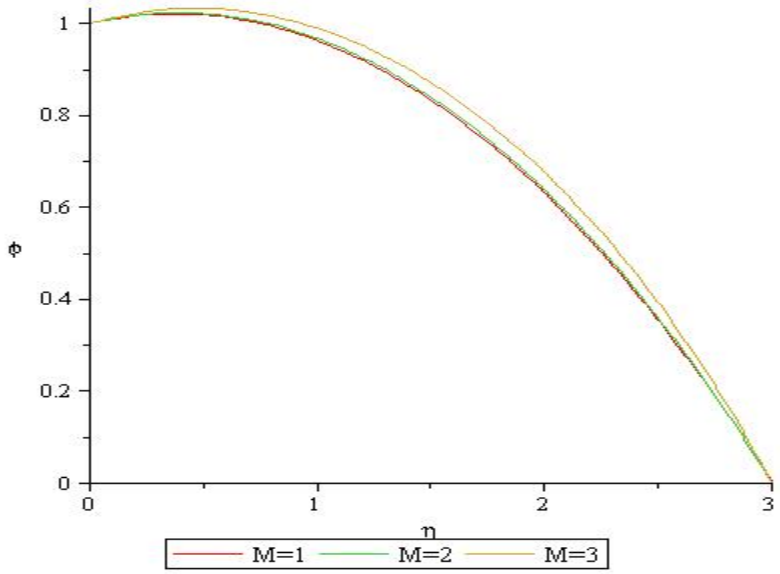

Figure 4.6: Variation of magnetic parameter on concentration profile with slip

Figures 4.4 to 4.6 are the variations of magnetic parameter on the velocity, temperature and concentration profiles respectively. As the magnetic parameter increases, the velocity profile reduces as a result of Lorentz force which is present while temperature and concentration all increases with increase in magnetic parameter. The magnetic parameter is a control parameter.

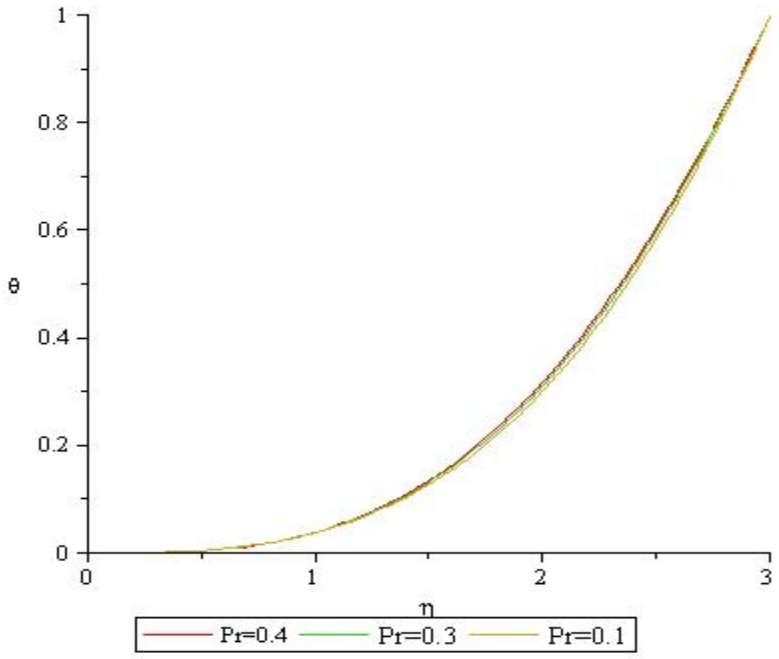

Figure 4.7: Variation of Prandtl number on temperature profile with slip

Figure 4.7 present the effects of Prandtl number on temperature profile. It is observe that as the Prandtl number increases, the fluid temperature reduces within the boundary layer before attaining maximum temperature.

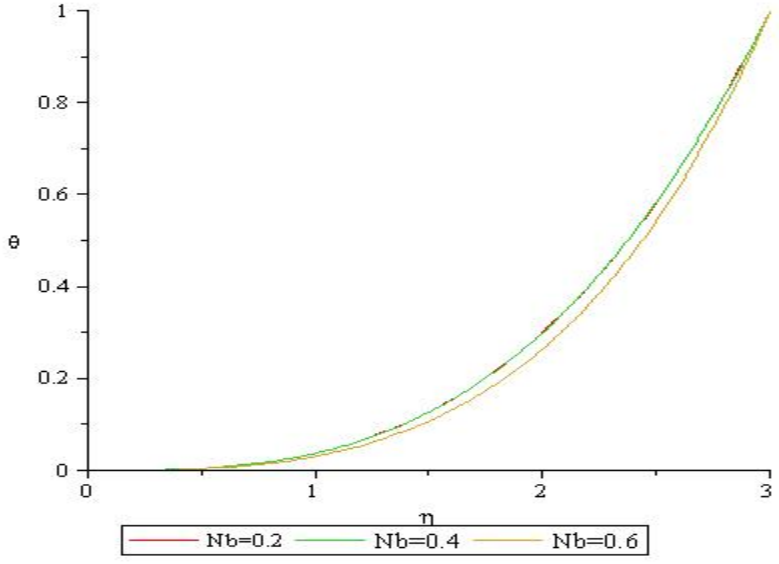

Figure 4.8: Variation of Brownian motion on temperature profile with slip

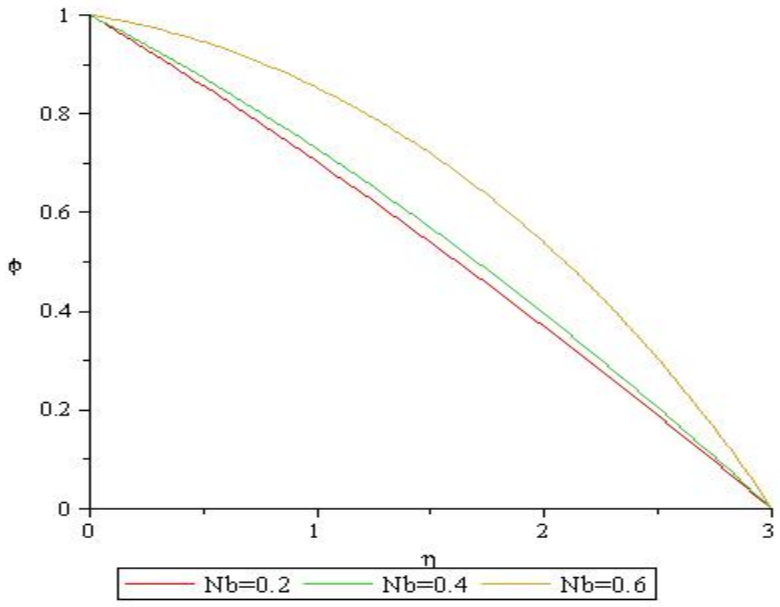

Figure 4.9: Variation of Brownian motion on concentration profile with slip

Figures 4.8 to 4.9 are the variation of Brownian motion on temperature and concentration profiles respectively. It is observe that as the Brownian motion increases, the fluid temperature also rises slightly, and concentration is also enhanced.

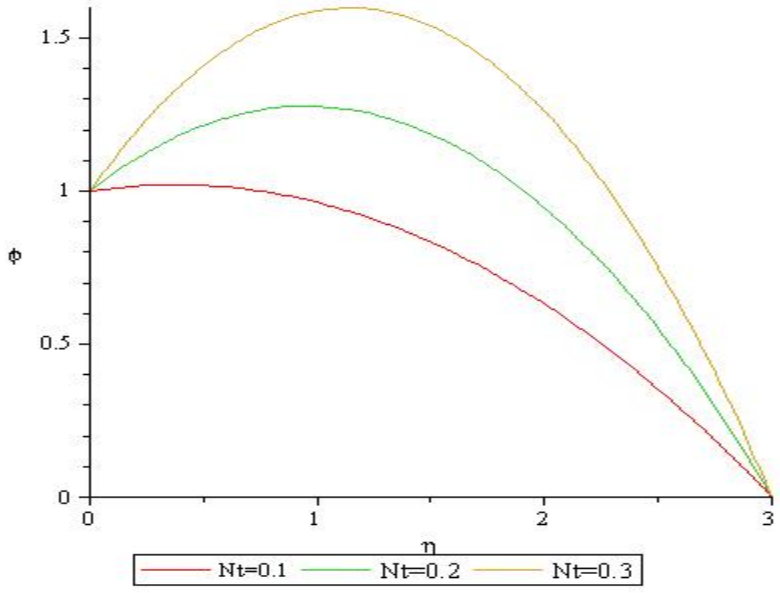

Figure 4.10: Variation of thermopheric parameter on concentration profile with slip

Figures 4.10 depict the variation of thermopheric parameter on concentration profile. It

is seen that thermopheric parameter act as a reduction agent to the concentration profile.

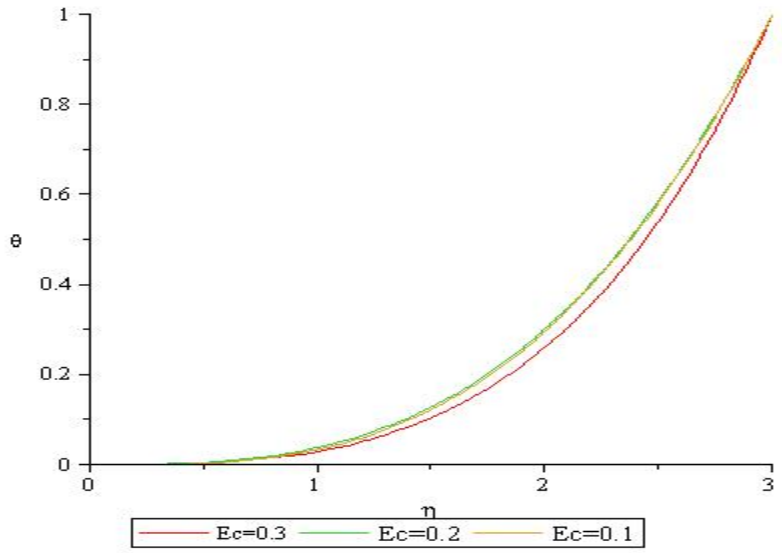

Figure 4.11: Variation of Eckert number on temperature profile with slip

Figure 4.11 is the variation of Eckert number on temperature profile. It is seen that the viscous term is an increasing agent of the temperature profile.

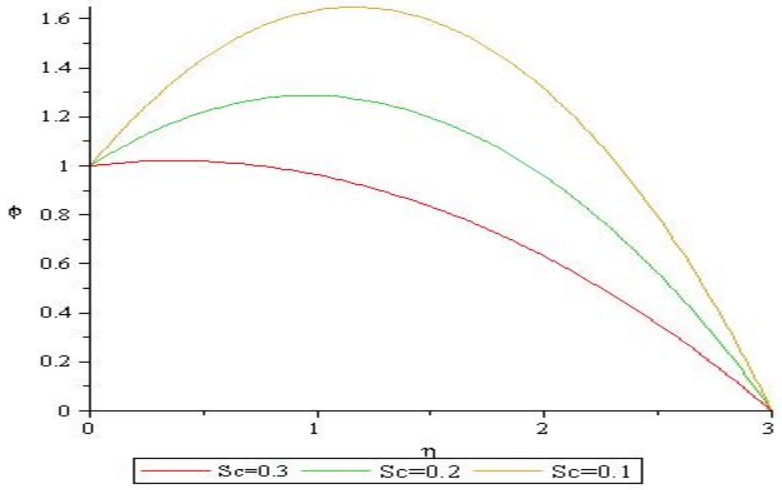

Figure 4.12: Variation of Schmidt number on concentration profile with slip

Figure 4.12 show the variation of Schmidt number on concentration profile. Schmidt number is seen clearly as a reduction agent to concentration profile.

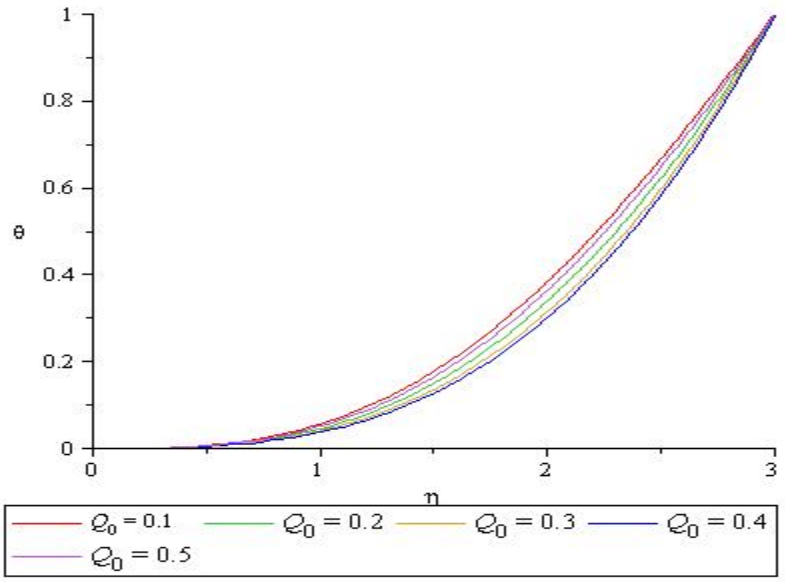

Figure 4.13: Variation of heat generation parameter on temperature profile with slip

Figure 4.13 depict the effects of heat generation parameter on the temperature profile. The heat generation is seen to increase the fluid temperature.

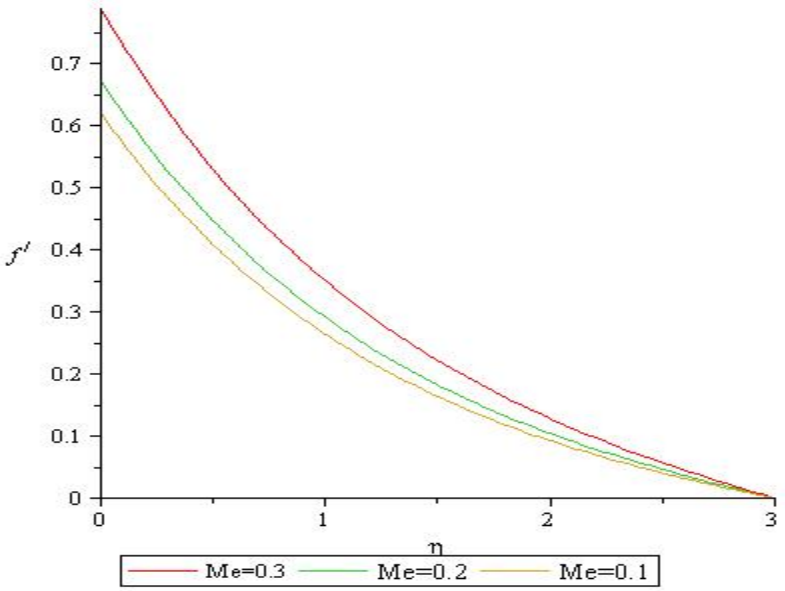

Figure 4.14: Variation of melting parameter on velocity profile with slip

Figure 4.14 present the effect of melting parameter on the velocity profile. It is observe that as the melting parameter increases, the fluid also rises on the melting surface before

attaining the free stream.

4.3 Presentation of Graphical Results for the Solution of Classical Problem of Nanofluid Flow

The graphical results for classical nanofluid with magnetic effects, porous medium, viscous dissipation and heat generation are presented as follows:

Figure 4.15 to 4.17 presents the variation of inverse Darcy number on velocity, temperature and concentration profile. As the inverse Darcy number increases, velocity profile is observed to be a reduction agent while the temperature and concentration appear as increasing agents.

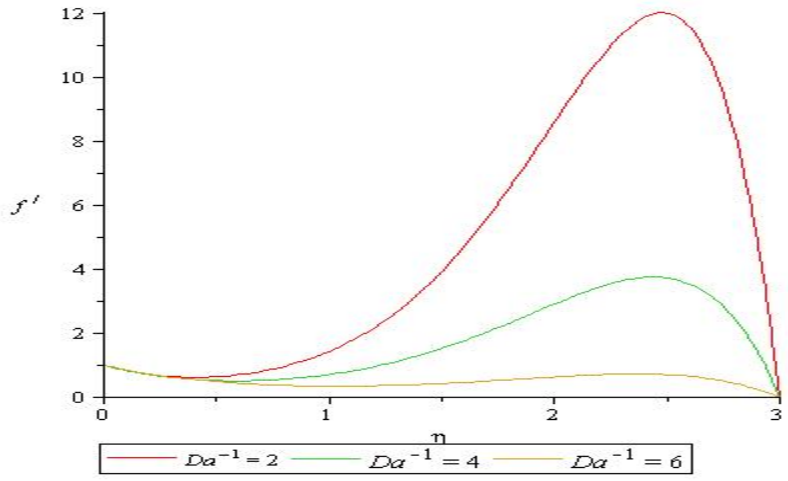

Figure 4.15: Variation of inverse Darcy number on velocity profile

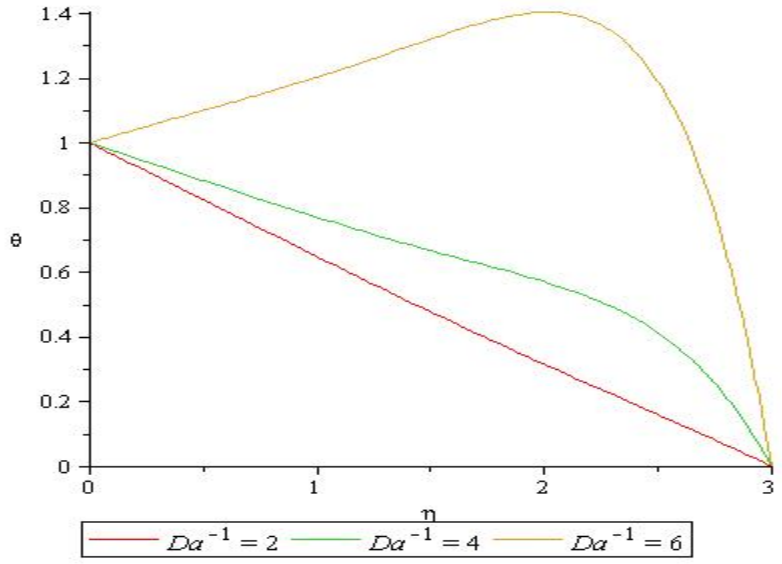

Figure 4.16: Variation of inverse Darcy number on temperature profile

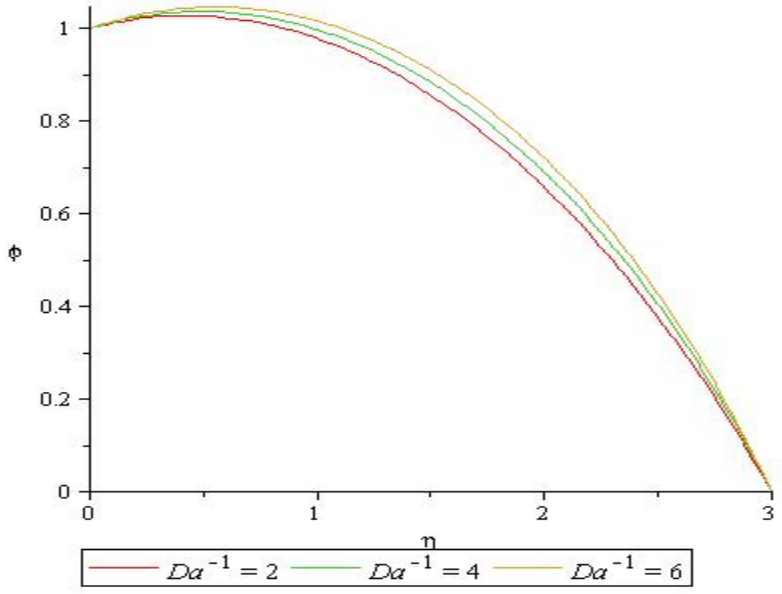

Figure 4.17: Variation of inverse Darcy number on concentration profile

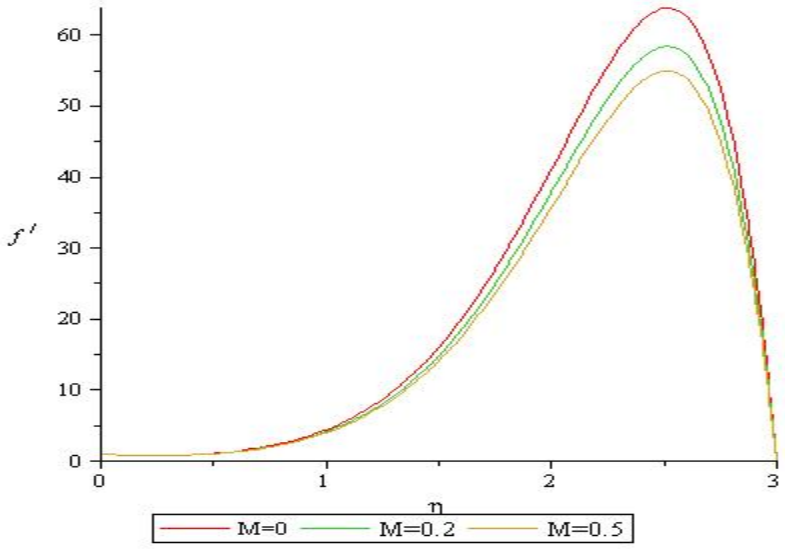

Figure 4.18: Variation of Magnetic number on velocity profile

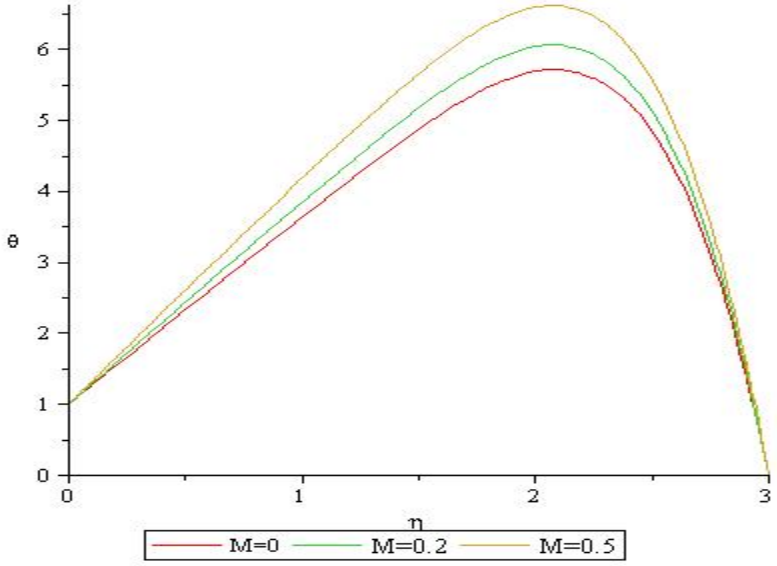

Figure 4.19: Variation of magnetic number on temperature profile

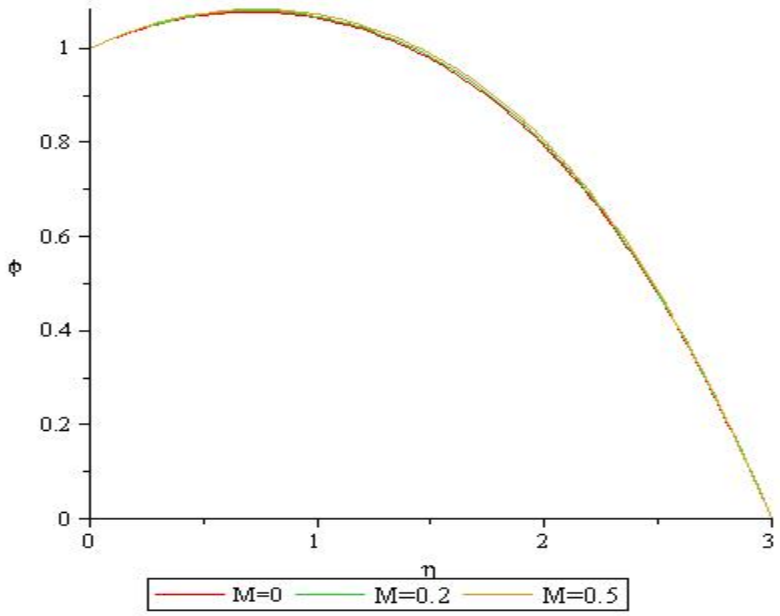

Figure 4.20: Variation of magnetic number on concentration profile

Figures 4.18 to 4.20 display the variation of magnetic number on velocity, temperature and concentration profile. As the magnetic increases, velocity profile is observed to drop due to drag like force. The temperature and concentration appear to be increasing as the magnetic parameter is enhance.

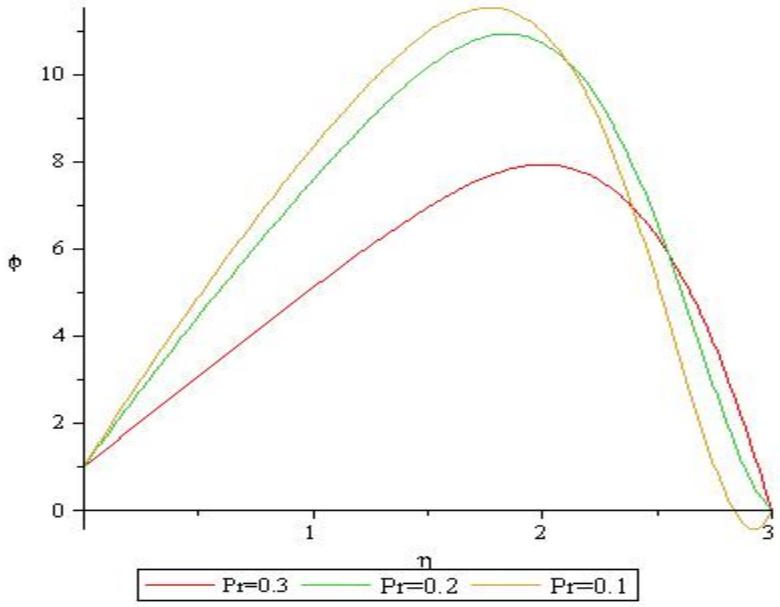

Figure 4.21: Variation of Prandtl number on temperature profile

Figure 4.21 show the variation of Prandtl number on the fluid temperature. The temperature of the fluid drops as the Prandtl number increases which can be use to regulate the fluid temperature.

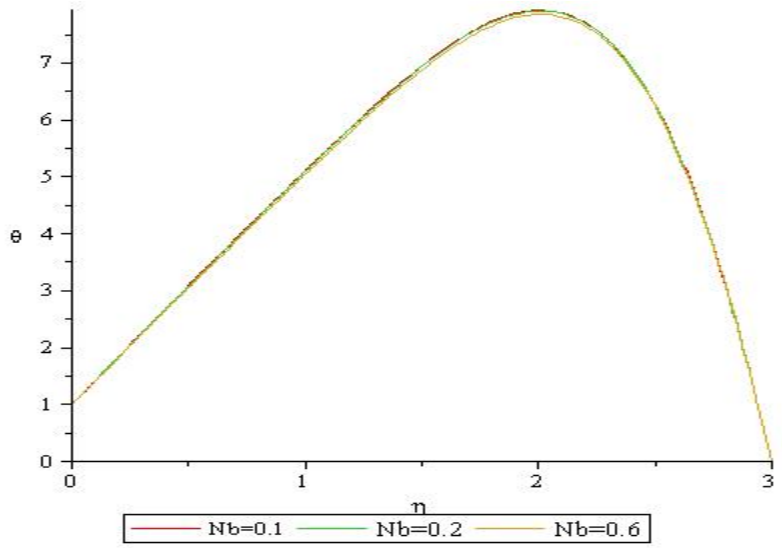

Figure 4.22: Variation of Brownian motion on temperature profil

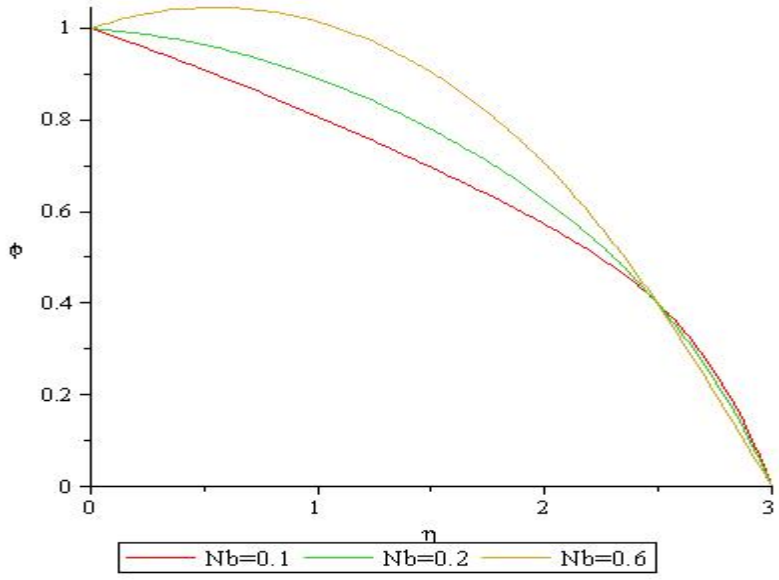

Figure 4.23: Variation of Brownian motion on concentration profile

Figures 4.22 to 4.23 are the graphs showing the variation of Brownian motion on temperature and concentration respectively. As the Brownian motion increases, the fluid temperature rises slightly and concentration also rises. On the concentration profile, as

the concentration approaches free stream $(\eta = 2.5)$ no changes was observed.

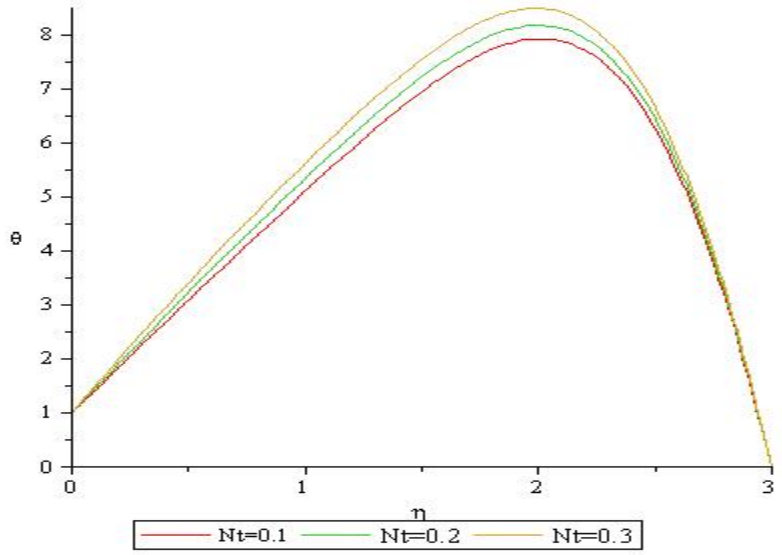

Figure 4.24: Variation of thermopheric parameter on temperature profile

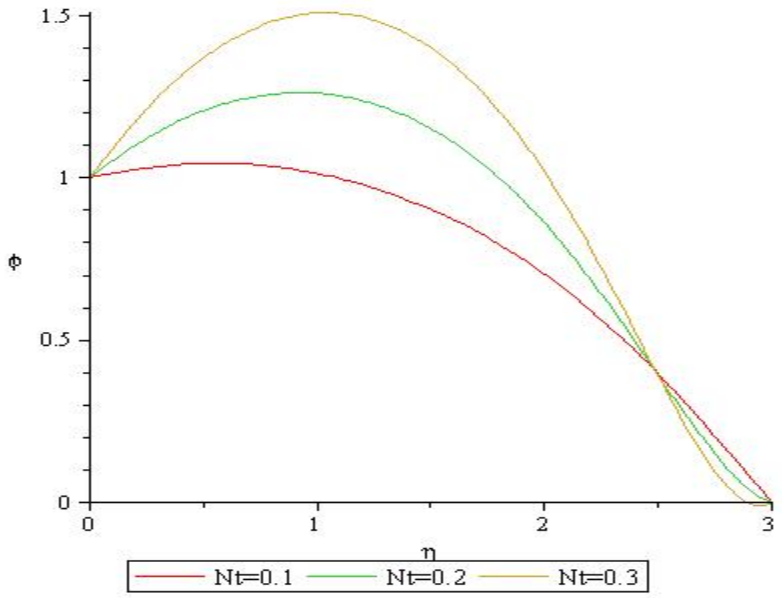

Figure 4.25: Variation of thermopheric parameter on concentration profile

Figures 4.24 to 4.25 depict the variation of thermopheric parameter on temperature and concentration profiles. As the thermopheric parameter rises, temperature and concentra tion profile all increases. No changes was observed on concentration profile at $\eta = 2.5$.

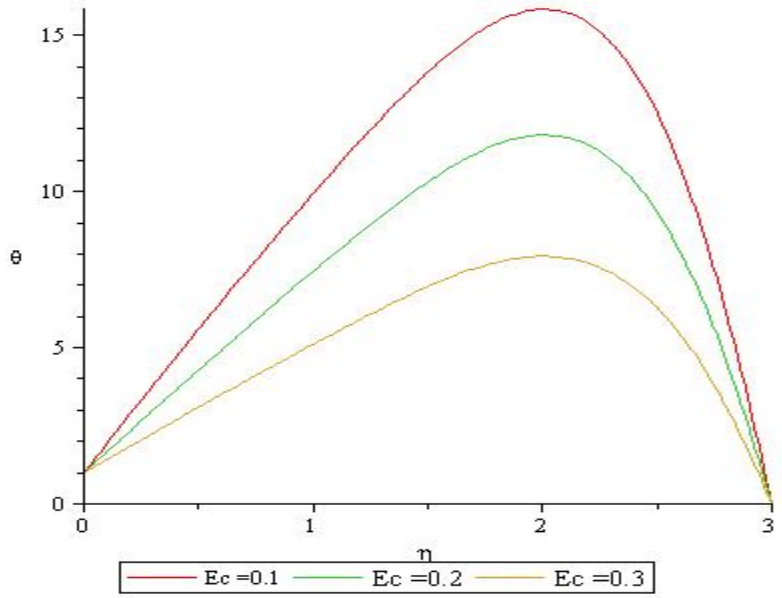

Figure 4.26: Variation of Eckert number on fluid temperature profile

Figure 4.26 is the variation of Eckert number on fluid temperature. It is seen that as the Eckert number increases the temperature profile also increases. This shows that the fluid temperature boundary thickness thickens as the fluid becomes more viscous.

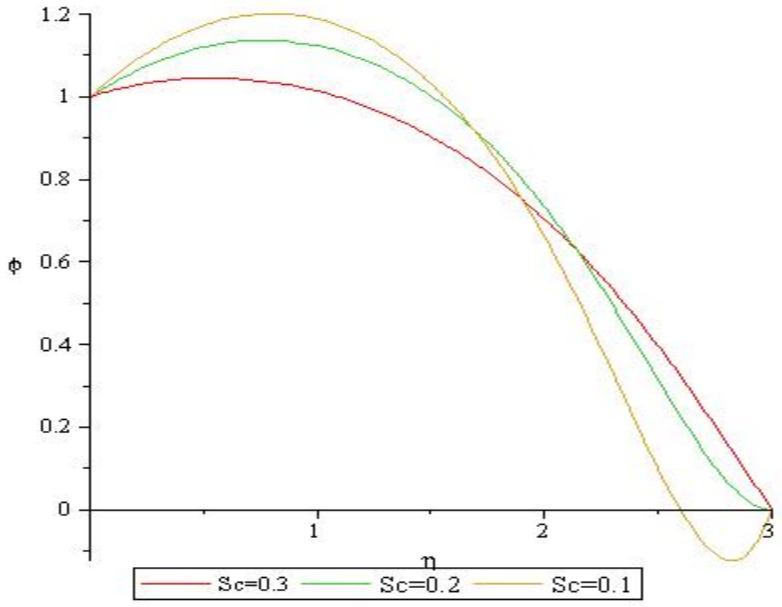

Figure 4.27: Variation of Schmdt number on concentration profile

Figure 4.27 present the variation of Schmdt number on concentration profile. It shows that the fluid concentration reduces as Schmdt number is enhanced.

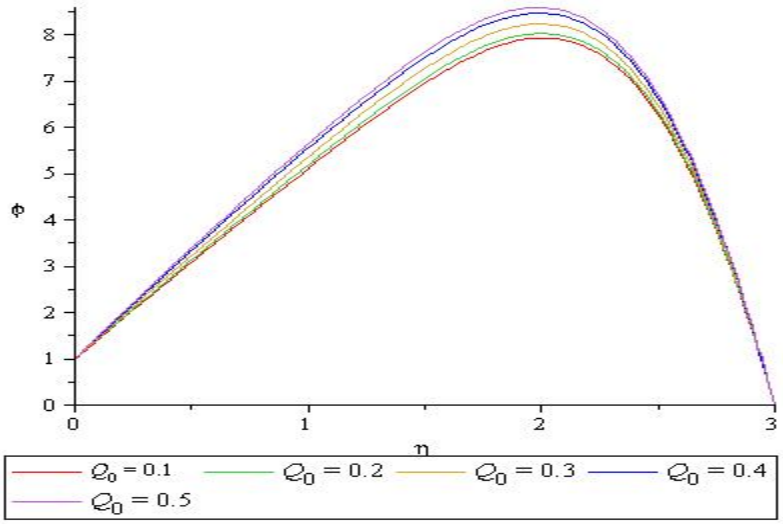

Figure 4.28: Variation of heat generation parameter on temperature profile

Figure 4.28 show the effects of heat generation on the temperature profile. As the heat generation number increase, the fluid temperature continue to increase.

CHAPTER FIVE

5.0 CONCLUSION AND RECOMMENDATIONS

5.1 Conclusion

This present work considered the work of previous literatures by in cooperating the porous medium and heat generation parameter. The problems formulated in rectangular system were transformed to nonlinear coupled ordinary differential equations. The non-linear coupled ordinary differential equations depends on some parameters such as magnetic parameter, melting parameter, Schmidt number, heat generation parameter, first and second slip parameters. The following observations were made:

i. The graphs presented in this work clearly satisfy the boundary conditions, which show the efficiency of the method.

ii. The results presented in this work were compared with the results of the existing literatures as seen in Table 4.1 and a good agreement was established which also signify the efficiency of the method used.

iii. At free stream, dimensionless distance is choosing to be at $\eta = 3$

iv. On the melting surface, the fluid velocity is not constant due to the slip parameters.

v. The fluid temperature is zero on the melting surface and takes some distance before it rises to maximum.

vi. This study present the results of the problems considered at all points (analytically).

5.2 Recommendations

The following recommendations were made:

i. Researchers are encouraged to extend the present study by adding more parameters and obtain the result of the problem using a different approach other than ADM.

ii. Subsequent studies are encouraged to consider the unsteady parts of the problems.

5.3 Contributions to Knowledge

The following contributions were made to knowledge:

1. The present work extends the work of Mabood *et al.* (2015) by introducing the porosity and heat generation terms and considered only the steady states of an incompressible nanofluid dynamics.
2. This study presents the results of the problems considered at all points (analytically) unlike the work of Mabood *et al*. (2015) which results were at mesh points.
3. It also reveals that Inverse Darcy number (1,2,4), Prandtl number (0.4,0.3,0.1) and Schmidt number (0.3,0.2,0.1) are seen as reduction agents to the fluid velocity, fluid temperature and concentration profile respectively. While the Melting parameter (0.3,0.2,0.1) are found to enhance the fluid velocity.

REFERENCES

Abu-Nada, E. & Chamkha, A. (2010). Effect of nanofluid variable properties on natural convection in enclosures filled with a CUO–water nanofluid. *International Journal of Thermal Science*, 4(9), 2339–2352.

Abdallah, A., Ibrahim, F. & Chamkha, A. (2018). Nonsimilar solution of unsteady mixed convection flow near the stagnation point of a heated vertical plate in a porous medium saturated with a nanofluid. *Journal of Porous Media,* 21(4), 363–388.

Adomian, G. (1994). Solving frontier problem of Physics: The Decomposition method. *Springer-Science +Business,* 6.

Andersson, H. (2002). Slip flow past a stretching surface. *Acta Mechanica.* 15(8), 121–145.

Awad, F. G., Sibanda, P. & Khidir, A. A. (2013). Thermodiffusion effects on magneto-nanofluid flow over a stretching sheet. *Boundary Value Problems*. 1(3), 6-56.

Besthapu, P. & Bandari, S. (2015). Mixed convection MHD Flow of a Casson nanofluid over a nonlinear permeable stretching sheet with viscous dissipation. *Journal of Applied Mathematical Physics*, 3(1), 1580–1593.

Buongiorno, J. (2006). Convective transport in nanofluids. *Journal of Heat Transfer,* 12(8), 240-250.

Choi, S. U. S. (1995). Enhancing thermal conductivity of fluids with nanoparticle, in D. A. Siginer, H. P. Wang (Eds.). *Developments and Applications of Non-Newtonian Flows*, 6(6), 99–105.

Congedo, P., Collura, S. & Congedo, P (2009). Modeling and analysis of natural convection of heat transfer in nanofluids. Heat Transfer Conference, Jacksonville. FL. 3(3), 569-579.

Cogley, A. C., Vincent, W. E. & Gilles, S. E. (1968). Differential approximation for radiation in a non-gray gas near equilibrium. *Non-analysis modelling and control,* 6, 551-553.

Crane, L. J. (1970). Flow past a stretching plate. *Zeitschrift fur Angewandte Mathematik und Physik*, 2(1), 64 - 75.

Fang, T., Lee, C. & Zhang, J. (2011). The boundary layers of an unsteady incompressible stagnation-point flow with mass transfer. *International Journal of Non-Linear Mechanics*, 46, 942–948.

Fang, T., Yao S., Zhang, J. & Aziz, A. (2010). Viscous flow over a shrinking sheet with a second order slip flow model. *Communications in Nonlinear Science and Numerical Simulation,* 15(1), 231–412.

Gbadeyan, J. A., Olanrewaju, M. A. & Olanrewaju P. O. (2011). Boundary layer flow of a nanofluid past a stretching sheet with a convective boundary condition in the presence of a magnetic field and thermal radiation. *Australian Journal of Basic Applied Sciences*, 5(13), 23–34.

Gireesha, B. J., Mahanthesh, B., Manjunatha, P. T. & Gorla, R .S. R (2015). Numerical solution for hydromagnetic boundary layer flow and heat transfer past a stretching surface embedded in non-darcy porous medium with fluid-particle suspension. *Journal of Nigeria Mathematical Society,* 3(4), 267–285.

Gorla, R.S.R. & Vasu, B. (2016). Unsteady convective heat transfer to a stretching surface in a non-newtonian nanofluid. *Journal of Nanofluids*, 5(3), 581–594.

Gorla, R.S.R., Vasu, B. & Siddiqa, S. (2016). Transient combined convective heat transfer over a stretching surface in a non-newtonian nanofluid using Buongiorno's model. *Journal of Applied Mathematical Physics,* 4(3), 443–460.

Hady, F., Ibrahim, F., Abdel-Gaid, S. & Eid. M. (2012a). Radiation effect on viscous flow of a nanofluid and heat transfer over a nonlinearly stretching sheet. *Nanoscale Residual Letters*. 7(3), 229–241.

Hady, F., Ibrahim, F., El-Hawary, H. & Abdelhady, A. (2012b). Effect of suction/injection on natural convective boundary-layer flow of a nanofluid past a vertical porous plate through a porous medium. *Journal of Modern Methods in Numerical Mathematics*, 3(2), 53–63.

Hamad, M., Pop, I. & Ismail, A. (2011). Magnetic field effects on free convection flow of a nanofluid past a semi-infinite vertical flat plate. *Nonlinear Analysis: Real World Application*, 1(2), 1338–1346.

Hassanien, I. & Al-Arabi, T. (2008). Thermal radiation and variable viscosity effects on unsteady mixed convection flow in the stagnation region on a vertical surface embedded in a porous medium with surface heat flux. *Far East Journal of Mathematical Science,* 2(8), 187–207.

Hassanien, I., Ibrahim, F. & Omer, G. (2004). Unsteady free convection flow in the stagnation-point region of a rotating sphere embedded in a porous medium. *Journal of Mechanical Engineering*, 7(1), 89–98.

Hassanien, I., Ibrahim F. & Omer, G. (2006). Unsteady flow and heat transfer of a viscous fluid in the stagnation region of a three-dimensional body embedded in a porous medium. *Journal of Porous Media*, 9(4), 357–372.

Hossain, M. A. & Takhar, H. S. (1996). Radiation effect on mixed convection along a vertical plate with uniform surface temperature. *Heat mass transfer*. 3(1), 243-248.

Ibrahim, W., Shankar, B. & Nandeppanavar, M. M. (2013). MHD stagnation point flow and heat transfer due to nanofluid towards a stretching sheet. *International Journal of Heat and Mass Transfer,* 5(6), 1–9.

Ishak, A., Nazar, R. & Pop, I. (2008). Dual solutions in mixed convection flow near a stagnation point on a vertical surface in a porous medium. *International Journal of Heat Mass Transfer*, 5(1), 1150–1155.

Kameswaran, P. K., Vasu, B., Murthy, P.V.S.N. & Gorla, R.S.R. (2016). Mixed convection from a wavy s urface embedded in a thermally stratified nanofluid

saturated porous medium with non-linear boussinesq approximation. *International Communication on Heat Mass Transfer,* 7(7), 78–86.

Khan, W. A. & Pop, I. (2010). Boundary layer flow of a nanofluid past a stretching sheet. *Int J Heat Mass Transfer*, 5(3), 2477–83.

Kumari, M., Takhar, H. & Nath, G. (1992). Unsteady mixed convection flow at the stagnation point. *International Journal of Engineering Sciences,* 30(12), 1789-1800.

Khanafer, K., Vafai, K. & Lightstone, M. (2003). Buoyancy-driven heat transfer enhancement in a two-dimensional enclosure utilizing nanofluids. *International Journal on Heat Mass Transfer,* 46(19), 3639-3653.

Li, D., Fotini, L. & Pop, I (2011). Mixed convection flow of a viscoelastic fluid near the orthogonal stagnation-point on a vertical surface. *International Journal of Sciences,* 50(9), 1698-1705.

Mabood, F. & Khan, W. (2014). Approximate analytic solutions for influence of heat transfer on MHD stagnation point flow in porous medium. *Computational Fluids*, 10(2), 72–78.

Mabood F, Khan W. A. & Ismail A. I. M. (2015). MHD boundary layer flow and heat transfer of nanofluids over a nonlinear stretching sheet: A numerical study. *Journal of Magnetism and Magnetic Materials*, 37(4), 569–76.

Mabood, F. & Mastroberardino, A. (2015). Melting heat transfer on MHD convective flow of a nanofluid over a stretching sheet with viscous dissipation and second order slip. *Journal of the Taiwan institute of Chemical engineers,* 17 (7), 1-7.

Mahapatra, T. R. & Gupta, A. G. (2002). Heat transfer in stagnation point flow towards a stretching sheet. *Heat Mass Transfer,* 3(8), 517–521.

Makinde, O. D. (2012). Heat and mass transfer by MHD mixed convection stagnation point flow toward a vertical plate embedded in a highly porous medium with radiation and internal heat generation. *Meccanica*, 4(7), 1173–1184.

Makinde O. D. & Aziz A. (2012). Boundary layer flow of a nanofluid past a stretching sheet with a convective boundary condition. *International Journal of Thermal Sciences,* 1(3), 26–32.

Makinde, O. D. (2005). Free convection flow with thermal radiation and mass transfer past a moving vertical porous plate. *International communication on Heat and Mass Transfer,* 2(5), 289-295.

Mustafa, M., Hayat, T. Pop, I., Asghar, S. & Obaidat, S. (2011), Stagnation-point flow of a nanofluid towards a stretching sheet, *International Journal of Heat and Mass Transfer,* 5(4), 5588-5594.

Nadeem, S. & Haq, R.U. (2013). Effect of thermal radiation for megnetohydrodynamic boundary layer flow of a nanofluid past a stretching sheet with convective boundary conditions, *Journal of Computational and Theoretical Nanoscience.* 1(1), 32–40.

Nadeem, S. & Lee, C. (2012). Boundary layer flow of nanofluid over an exponentially stretching surface. *Nanoscale Research Letters,* 7 (1), 94 -121.

Nandeppanavar, M. M., Vajravelu, K., Abel, M. S. & Siddalingappa, M. N. (2012). Second order slip flow and heat transfer over a stretching sheet with non-linear Navier boundary condition. *International Journal of Thermal Sciences*. 5(1), 43–50.

Nield, D. A. & Kuznetsov, A. V. (2009). The Cheng-Minkowycz problem for natural convective boundary-layer flow in a porous medium saturated by nanofluid. *International Journal of Heat and Mass Transfer.* 5(2), 5792–5795.

Rana, P. & Bhargava, R. (2012). Flow and heat transfer of a nanofluid over a nonlinaely stretching sheet: A numerical study. *Communications in Nonlinear Science and Numerical Simulation.* 17, 212-226.

Ramachandra, N. & Chen, T. S. (1988). Mixed convection in stagnation flows adjacent to vertical surfaces. *Journal of Heat Transfer*. 110(2), 373-377.

Rosali, H., Ishak, A., Nazar, R. & Merkin, J. H. (2014). The effect of unsteadiness on mixed convection boundary-layer stagnation-point flow over a vertical flat surface embedded in a porous medium. *International Journal of Heat and Mass Transfer.* 77, 147-156.

Rudraswamy, N. G. & Gireesha, B. J. (2015). MHD Flow and Heat Transfer of a Nanofluid Embedded with Dust particles over a stretching sheet. *Journal of Nanofluids*. 66-72.

Sakiadis, B. C. (1961). Boundary layer behaviour on continuous solid surface: II-boundary layer on a continuous flat surface. *American Institute of Chemical Engineers*. 7(2), 22- 45.

Satter, M. D. A. & Hamid, M. D. K. (1996). Unsteady free convection interaction with thermal radiation in a boundary layer flow past a vertical porous plate. *Journal of Mathematical Physics Science.* 30(2), 25-37.

Seshadri, R., Sreeshylan, N. & Nath, G. (2002). Unsteady mixed convection flow in the stagnation region of a heated vertical plate due to impulsive nature. *International Journal of Heat and Mass Transfer.* 45(6), 1345-1352.

Shateyi, S. & Marewo, G. T. (2014). Numerical analysis of unsteady MHD flow near a stagnation point of a two-dimensional porous body with heat and mass transfer Thermal Radiation, and Chemical Reaction. *Boundary Value Problem*, 218.

Sheikholeslami, M., Abelma, S. & Ganji, D. D. (2014). Numerical simulation of MHD nanofluid flow and heat transfer considering viscous dissipation. *International Journal of Heat and Mass Transfer.* 79, 212-222.

Sheikholeslami, M. & Ganji, D. D. (2015). Entropy generation of nanofluid in presence of magnetic field using Lattice Boltzmann method. *Physica A.* 41(7), 273–286.

Siddiqa, S., Begum, N., Hossain, M. A. & Gorla, R.S.R (2016a). Numerical solutions of natural convection flow of a dusty nanofluid about a vertical wavy truncated cone. *Journal of Heat Transfer.* 13(9), 022-503.

Siddiqa, S., Sulaiman, M., Hossain, M.A., Islam, S. & Gorla, R.S.R. (2016b). Gyrotactic bioconvection flow of a nanofluid past a vertical wavy surface. *International Journal of Thermal Science*. 10(8), 244–250.

Srinivasacharya, D. & Surender, O. (2014). Non-similar solution for natural convective boundary layer flow of a nanofluid past a vertical plate embedded in a doubly stratified porous medium. *Journal of Heat Mass Transfer*. 7(1), 431–438.

Vasu, B. & Manish, K. (2015). Transient boundary layer laminar free convective flow of a nanofluid over a vertical cone/plate. *International Journal of Applied Computational Mathematics*. 1(2), 427–448.

Wu, L. (2008). A slip model for rarefied gas flows at arbitrary Kundsen number. *Applied Physics Letters*. 9(3), 25- 103.

Yacob, N., Ishak, A. & Pop, I. (2011). Falkner–Skan problem for a static or moving wedge in nanofluids. *International Journal of Thermal Sciences*, 5(2), 133–139.

Yoshimura, A. & Prudhomme, R. K. (1988). Wall slip corrections for Couette and parallel flow viscometers. *Journal of Rheology*. 3(2), 53–67.

Yusuf, A., Bolarin, G. & Adekunle, S. T (2019). Analytical Solution of unsteady Boundary Layer Flow of a nanofluid past a Stretching inclined sheet with effect of magnetic Field. *FUOYE Journal of Engineering and Technology (FUOYEJET).* 4(1), 97-101.

Yusuf, A., Bolarin, G., Jiya, M. & Aiyisimi, Y. M. (2018). Boundary layer flow of a nanofluid in an inclined wavy wall with convective boundary condition. *Communication in Mathematical Modeling and Applications.* 3(4), 48-56.

Zaimi, K., Ishak, A. & Pop, I. (2014). Unsteady flow due to a contracting cylinder in a nanofluid using Buongiorno's model. *International Journal of Heat and Mass Transfer*, 6(8), 509–513.

Zhang, T., Jia, L. & Wang, Z. (2008). Validation of the Navier-Stokes equation for the slip flow analysis within transition region. *International Journal of Heat and Mass Transfer.* 5(1), 623–712.

APPENDIX A (Solution to Equation 3.9)

$$
\begin{aligned}
f(\eta) := {} & -10.\,Me\,b1 + \eta\,(1 + 0.1\,a + 0.1\,b) - 1.589024858\eta^2 \\
& + 1.683333333\eta^3 - 5.296749527 Me\,b1\,\eta^3 + 0.1683333333a\,\eta^3 \\
& + 0.1683333333b\,\eta^3 + 0.1324187382\eta^4\,(1. + 0.1000000000a \\
& + 0.1000000000b) - 1.337429255\eta^4 + 0.7659166664\eta^5 \\
& - 0.0005192382640(1. + 0.1000000000a + 0.1000000000b \\
& - 3.178049716\eta)^5 - 0.1748102155 Me\,b1\,(1. \\
& + 0.1000000000a + 0.1000000000b)^3\,\eta^3 + 0.08500833330a\,\eta^5 \\
& + 0.08500833330b\,\eta^5 - 0.4056868740\eta^6 \\
& - 2.674858512 Me\,b1\,\eta^5 - 0.00001236281581(1. \\
& + 0.1000000000a + 0.1000000000b - 3.178049716\eta)^7 \\
& - 0.04048015871\eta^7 + 0.04458097520\eta^6\,(1. + 0.1000000000a \\
& + 0.1000000000b) + 0.004458097517a\,\eta^6 \\
& + 0.004458097517b\,\eta^6 - 0.004761904761(29.71083332 \\
& + 0.4208333335a + 0.4208333335b)\,\eta^7 \\
& - 0.008333333333(33.66666665 Me\,b1 + (1. + 0.1000000000a \\
& + 0.1000000000b)\,(-17.63817592 - 0.1589024859a \\
& - 0.1589024859b) + 0.1666666667(1. + 0.1000000000a \\
& + 0.1000000000b)\,(-6.356099432 - 0.6356099432a \\
& - 0.6356099432b) - 0.5296749528(1. + 0.1000000000a \\
& + 0.1000000000b)^2 - 1.604915107b - 1.604915107a \\
& - 16.04915107)\,\eta^6 - 0.01666666666(-10.\,Me\,b1\,(\\
& -17.63817592 - 0.1589024859a - 0.1589024859b) + (1. \\
& + 0.1000000000a + 0.1000000000b)\,(-0.1048861293(1. \\
& + 0.1000000000a + 0.1000000000b)\,(-6.356099432 \\
& - 0.6356099432a - 0.6356099432b) + 0.3333333334(1. \\
& + 0.1000000000a + 0.1000000000b)^2 + 1.010000000b \\
& - 31.78049716 Me\,b1 + 1.010000000a + 10.10000000) \\
& + 0.1666666667(1. + 0.1000000000a + 0.1000000000b)^3)\,\eta^5 \\
& - 0.04166666668(-10.\,Me\,b1\,(-0.1048861293(1. \\
& + 0.1000000000a + 0.1000000000b)\,(-6.356099432 \\
& - 0.6356099432a - 0.6356099432b) + 0.3333333334(1. \\
& + 0.1000000000a + 0.1000000000b)^2 + 1.010000000b \\
& - 31.78049716 Me\,b1 + 1.010000000a + 10.10000000) \\
& - 0.1048861293(1. + 0.1000000000a + 0.1000000000b)^4)
\end{aligned}
$$

$$
\begin{aligned}
\theta(\eta) := {} & -0.05050000000\eta^2 + b1\,\eta^3 + 0.1069943404\eta^3 \\
& - 0.002500000000b1\,\eta^4\,c1 - 0.005000000000Q_0\,b1\,\eta^5 \\
& - 0.003000000000b1^2\,\eta^6 - 0.3000000000b1\,\big(\\
& -0.05296749527\eta^6 + 0.05000000000\eta^5\,(1. + 0.1000000000a \\
& + 0.1000000000b) - 0.8333333332Me\,b1\,\eta^4\big) \\
& - 0.3535000000Me\,b1\,\eta^3 + 0.01069943404a\,\eta^3 \\
& + 0.01069943404b\,\eta^3 + 0.008416666668\eta^4\,(1. \\
& + 0.1000000000a + 0.1000000000b) - 0.08500833325\eta^4 \\
& - 0.005349717020\eta^5 - 0.00003300330034\big(1. \\
& + 0.1000000000a + 0.1000000000b - 3.178049716\eta\big)^5 \\
& - 0.3000000000b1\,\big(0.001168981482\eta^9 + 0.01785714286(\\
& -1.469847993 - 0.01324187382a - 0.01324187382b)\,\eta^8 \\
& + 0.02380952381\big(-5.296749527Me\,b1 + 1.683333333 \\
& - 0.0005192382640(1. + 0.1000000000a + 0.1000000000b)\,(\\
& -128.3932085 - 12.83932085a - 12.83932085b) \\
& + 0.03333333334(1. + 0.1000000000a + 0.1000000000b)^2 \\
& + 0.001650165017(-6.356099432 - 0.6356099432a \\
& - 0.6356099432b)^2 + 0.1683333333b + 0.1683333333a\big)\,\eta^7 \\
& + 0.03333333333\big(-0.0005192382640(1. + 0.1000000000a \\
& + 0.1000000000b)\,\big(20.19999999(1. + 0.1000000000a \\
& + 0.1000000000b)^2 + (-6.356099432 - 0.6356099432a \\
& - 0.6356099432b)^2\big) + 0.003300330035(1. \\
& + 0.1000000000a + 0.1000000000b)^2\,(-6.356099432 \\
& - 0.6356099432a - 0.6356099432b)\big)\,\eta^6 + 0.05000000000\big(\\
& -0.001038476528(1. + 0.1000000000a + 0.1000000000b)^3\,(\\
& -6.356099432 - 0.6356099432a - 0.6356099432b) \\
& + 0.001650165017(1. + 0.1000000000a + 0.1000000000b)^4\big)\,\eta^5 \\
& - 0.00004326985532(1. + 0.1000000000a \\
& + 0.1000000000b)^5\,\eta^4\big) - 0.001388888889\big(0.02860244744b1^2 \\
& - 0.1515000000b1\big)\,\eta^9 - 0.001785714286\big((1. \\
& + 0.1000000000a + 0.1000000000b)\,\big(-0.01800000000b1^2 \\
& + 0.09534149148b1\big) + 0.4767074574b1\,(0.2500000000 \\
& + 0.02500000000a + 0.02500000000b) \\
& + 0.03972562145Q_0\,b1\big)
\end{aligned}
$$

$$
\begin{aligned}
\phi(\eta) := {} & 1 + c1\,\eta - 0.1000000000\,c1\,\left(0.1666666667\,\eta^3\,(1.\right. \\
& + 0.1000000000\,a + 0.1000000000\,b) - 0.1324187382\,\eta^4 \\
& \left. - 5.\,Me\,b1\,\eta^2\right) - 0.1000000000\,\eta^2 \\
& - 0.1000000000\,c1\,\left(0.004413957940\,\eta^6\,(1. + 0.1000000000\,a\right. \\
& \left. + 0.1000000000\,b) - 0.002003968253\,\eta^7\right. \\
& - 0.2648374764\,Me\,b1\,\eta^5 - 0.000001224041170\,(1. \\
& + 0.1000000000\,a + 0.1000000000\,b - 3.178049716\,\eta)^7 \\
& + 0.08416666664\,\eta^5 + 0.008416666664\,a\,\eta^5 \\
& \left. + 0.008416666664\,b\,\eta^5 - 0.04458097517\,\eta^6\right) \\
& + 0.0002003968254\,c1\,\eta^7 - 0.003333333333\,(0.05296749528\,(1. \\
& + 0.1000000000\,a + 0.1000000000\,b)\,c1 \\
& + 0.1589024858\,c1\,(0.5000000001 + 0.05000000001\,a \\
& + 0.05000000001\,b))\,\eta^6 - 0.005000000000\,(\\
& - 2.118699811\,c1\,Me\,b1 - 0.1000000000\,(1. + 0.1000000000\,a \\
& + 0.1000000000\,b)\,c1\,(0.5000000001 + 0.05000000001\,a \\
& + 0.05000000001\,b) + 0.1589024858)\,\eta^5 \\
& - 0.008333333332\,(Me\,b1\,c1\,(0.5000000001 + 0.05000000001\,a \\
& + 0.05000000001\,b) + (1. + 0.1000000000\,a \\
& + 0.1000000000\,b)\,(c1\,Me\,b1 - 0.1000000000))\,\eta^4 \\
& + 0.1666666667\,Me\,b1\,(c1\,Me\,b1 - 0.1000000000)\,\eta^3
\end{aligned}
$$

APPENDIX B (Solution to Equation 3.10)

$$
\begin{aligned}
f(\eta) :=& \eta - \frac{1}{2}\, a \sqrt{M + \frac{1}{Da}}\ \eta^2 + a \sqrt{M + \frac{1}{Da}} \left(\frac{1}{24}\, \eta^4 \right. \\
& \left. - \frac{1}{120}\, a \sqrt{M + \frac{1}{Da}}\ \eta^5 \right) - \frac{1}{60}\, \frac{\left(1 - a \sqrt{M + \frac{1}{Da}}\ \eta\right)^5}{a^3 \left(M + \frac{1}{Da}\right)^{3/2}} \\
& + \left(M + \frac{1}{Da}\right) \left(\frac{1}{6}\, \eta^3 - \frac{1}{24}\, a \sqrt{M + \frac{1}{Da}}\ \eta^4 \right) \\
& - \frac{1}{48}\, \frac{\eta^4}{a \sqrt{M + \frac{1}{Da}}} \\
& + a \sqrt{M + \frac{1}{Da}} \left(a \sqrt{M + \frac{1}{Da}} \left(\frac{1}{5040}\, \eta^7 \right. \right. \\
& \left. - \frac{1}{40320}\, a \sqrt{M + \frac{1}{Da}}\ \eta^8 \right) \\
& + \frac{1}{20160}\, \frac{\left(1 - a \sqrt{M + \frac{1}{Da}}\ \eta\right)^8}{a^6 \left(M + \frac{1}{Da}\right)^3} + \left(M \right. \\
& \left. \left. + \frac{1}{Da} \right) \left(\frac{1}{720}\, \eta^6 - \frac{1}{5040}\, a \sqrt{M + \frac{1}{Da}}\ \eta^7 \right) \right) \\
& + \frac{1}{36}\, \frac{\eta^3}{a^2 \left(M + \frac{1}{Da}\right)} - \frac{1}{210} \left(\frac{1}{6}\, a^2 \left(M + \frac{1}{Da}\right) \right. \\
& - \frac{1}{2}\, a \sqrt{M + \frac{1}{Da}} \left(-\frac{1}{2}\, a \sqrt{M + \frac{1}{Da}} - \frac{1}{2} \left(M \right. \right. \\
& \left. \left. + \frac{1}{Da} \right)^{3/2} a \right) \Bigg) \eta^7 - \frac{1}{120} \left(-\frac{1}{2}\, a \sqrt{M + \frac{1}{Da}} \right. \\
& - \frac{1}{2} \left(M + \frac{1}{Da}\right)^{3/2} a - \frac{1}{2}\, a \sqrt{M + \frac{1}{Da}} \left(1 + M \right. \\
& \left. \left. + \frac{1}{Da} \right) \right) \eta^6 - \frac{1}{60} \left(\frac{7}{6} + M + \frac{1}{Da} \right) \eta^5 \\
& + \frac{1}{105} \left(\frac{1}{24}\, a^2 \left(M + \frac{1}{Da}\right) - a \sqrt{M + \frac{1}{Da}} \left(\right. \right. \\
& \left. \left. - \frac{1}{6}\, a \sqrt{M + \frac{1}{Da}} - \frac{1}{6} \left(M + \frac{1}{Da}\right)^{3/2} a \right) \right)
\end{aligned}
$$

$$\theta(\eta) := 1 + b1\,\eta - P_r\,b1\left(\frac{1}{6}\eta^3 - \frac{1}{24}\,a\sqrt{M+\frac{1}{Da}}\,\eta^4\right)$$
$$-\frac{1}{2}P_r E_c a^2\left(M+\frac{1}{Da}\right)\eta^2 - \frac{1}{2}N_b P_r\,b1\,c1\,\eta^2$$
$$-\frac{1}{2}N_t P_r\,b1^2\,\eta^2 - Q_0 P_r\left(\frac{1}{2}\eta^2 + \frac{1}{6}b1\,\eta^3\right)$$
$$-P_r\left(b1\left(a\sqrt{M+\frac{1}{Da}}\left(\frac{1}{720}\eta^6\right.\right.\right.$$
$$\left.\left.\left.-\frac{1}{5040}\,a\sqrt{M+\frac{1}{Da}}\,\eta^7\right)\right.\right.$$
$$-\frac{1}{2520}\,\frac{\left(1-a\sqrt{M+\frac{1}{Da}}\,\eta\right)^7}{a^5\left(M+\frac{1}{Da}\right)^{5/2}} + \left(M+\frac{1}{Da}\right)\left(\frac{1}{120}\eta^5\right.$$
$$\left.\left.-\frac{1}{720}\,a\sqrt{M+\frac{1}{Da}}\,\eta^6\right)\right) - \frac{1}{504}\,a^2\left(M+\frac{1}{Da}\right)P_r\,b1\,\eta^7$$
$$+\frac{1}{30}\left(\frac{1}{6}P_r\,b1\,a\sqrt{M+\frac{1}{Da}} - \frac{1}{2}\,a\sqrt{M+\frac{1}{Da}}\left(\right.\right.$$
$$\left.\left.-\frac{1}{2}P_r\,b1 - \frac{1}{2}Q_0 P_r\,b1\right)\right)\eta^6 + \frac{1}{20}\left(-\frac{1}{2}P_r\,b1\right.$$
$$-\frac{1}{2}Q_0 P_r\,b1 - \frac{1}{2}\,a\sqrt{M+\frac{1}{Da}}\left(-N_t P_r\,b1^2 - Q_0 P_r\right.$$
$$\left.\left.-P_r E_c a^2\left(M+\frac{1}{Da}\right) - N_b P_r\,b1\,c1\right)\right)\eta^5 + \frac{1}{12}\left(\right.$$
$$\left.-N_t P_r\,b1^2 - Q_0 P_r - P_r E_c a^2\left(M+\frac{1}{Da}\right) - N_b P_r\,b1\,c1\right)$$
$$\left.\eta^4\right) + 2\,P_r E_c\,a\sqrt{M+\frac{1}{Da}}\left(a\sqrt{M+\frac{1}{Da}}\left(\frac{1}{24}\eta^4\right.\right.$$
$$\left.\left.-\frac{1}{120}\,a\sqrt{M+\frac{1}{Da}}\,\eta^5\right) - \frac{1}{60}\,\frac{\left(1-a\sqrt{M+\frac{1}{Da}}\,\eta\right)^5}{a^3\left(M+\frac{1}{Da}\right)^{3/2}}\right.$$
$$\left.+\left(M+\frac{1}{Da}\right)\left(\frac{1}{6}\eta^3 - \frac{1}{24}\,a\sqrt{M+\frac{1}{Da}}\,\eta^4\right)\right)$$

$$\phi(\eta) := 1 + c1\,\eta - S_c\,c1\left(\frac{1}{6}\eta^3 - \frac{1}{24}\,a\sqrt{M+\frac{1}{Da}}\,\eta^4\right)$$

$$- S_c\left(c1\left(a\sqrt{M+\frac{1}{Da}}\left(\frac{1}{720}\eta^6\right.\right.\right.$$

$$\left.\left.\left. - \frac{1}{5040}\,a\sqrt{M+\frac{1}{Da}}\,\eta^7\right)\right.\right.$$

$$\left. - \frac{1}{2520}\,\frac{\left(1 - a\sqrt{M+\frac{1}{Da}}\,\eta\right)^7}{a^5\left(M+\frac{1}{Da}\right)^{5/2}} + \left(M+\frac{1}{Da}\right)\left(\frac{1}{120}\eta^5\right.\right.$$

$$\left.\left. - \frac{1}{720}\,a\sqrt{M+\frac{1}{Da}}\,\eta^6\right)\right) - S_c\,c1\left(\frac{1}{504}\,a^2\left(M\right.\right.$$

$$\left.\left. + \frac{1}{Da}\right)\eta^7 - \frac{1}{72}\,a\sqrt{M+\frac{1}{Da}}\,\eta^6 + \frac{1}{40}\eta^5\right)\Bigg)$$

$$+\left(c1\left(a\sqrt{M+\frac{1}{Da}}\left(\frac{1}{720}\eta^6 - \frac{1}{5040}\,a\sqrt{M+\frac{1}{Da}}\,\eta^7\right)\right.\right.$$

$$\left. - \frac{1}{2520}\,\frac{\left(1 - a\sqrt{M+\frac{1}{Da}}\,\eta\right)^7}{a^5\left(M+\frac{1}{Da}\right)^{5/2}} + \left(M+\frac{1}{Da}\right)\left(\frac{1}{120}\eta^5\right.\right.$$

$$\left.\left. - \frac{1}{720}\,a\sqrt{M+\frac{1}{Da}}\,\eta^6\right)\right) - S_c\,c1\left(\frac{1}{504}\,a^2\left(M\right.\right.$$

$$\left.\left. + \frac{1}{Da}\right)\eta^7 - \frac{1}{72}\,a\sqrt{M+\frac{1}{Da}}\,\eta^6 + \frac{1}{40}\eta^5\right)\Bigg) - S_c$$